

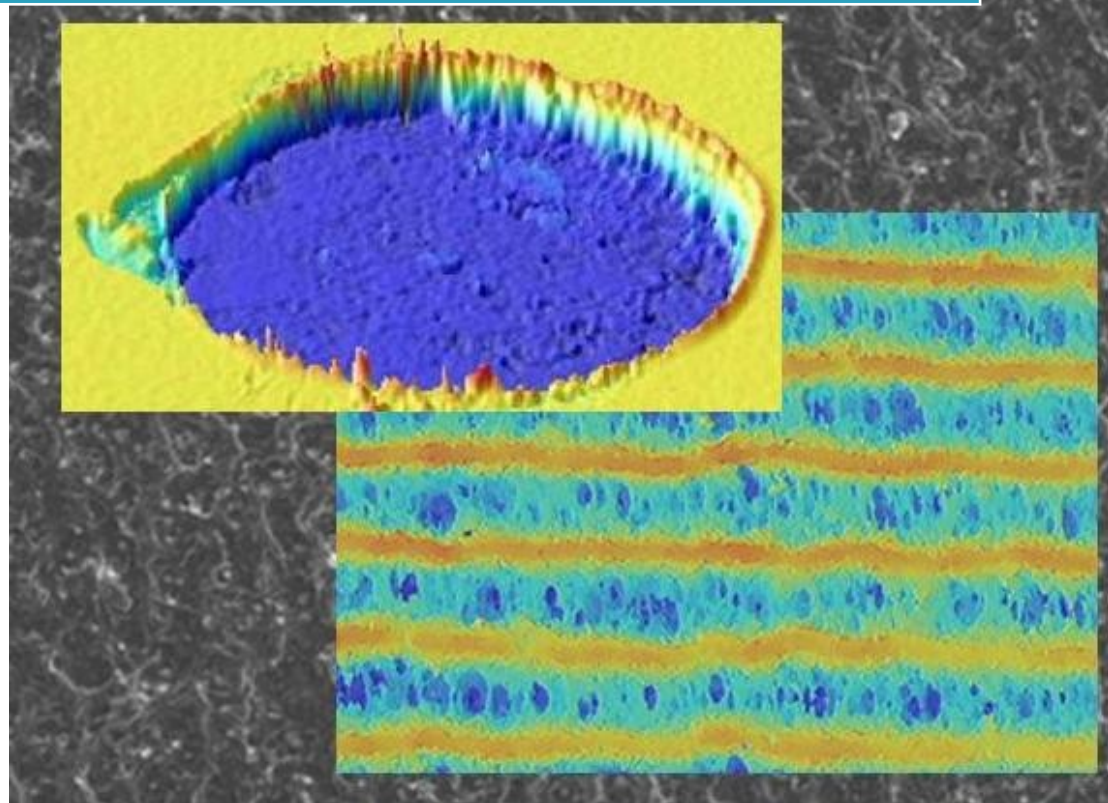


Facultad de Ciencias
Universidad Zaragoza



**Master in Physics
and Physical
Technologies**

LASER MARKING OF POLYMERS WORK METHODOLOGY



Directors:

José Ignacio Peña

Luis Oriol

Author:

Luis Villarreal

Special thanks to Ander Villate (B.S.H. Vitoria), Naira Soguero (B.S.H. Vitoria), Carlos Sánchez (group of liquid crystals and polymers), Francisco Ester (B.S.H. Zaragoza), Andrés Escartín (B.S.H. Zaragoza) and Ingke Masthoff.

TABLE OF CONTENTS

Table of contents

1 Introduction	1
2 Aim of the work	1
3 State of art	2-5
3.1 Research articles	
3.2 Patents	
3.3 Information provided by industries	
4 Photochemical and photothermal	6
5 Design of experiments (DoE)	7
6 Preparation of samples	8-9
6.1 Introduction	
6.2 Polymer films	
6.3 Bulk	
7 Temperature	10
7.1 Introduction	
7.2 Pyrometer	
7.3 Mathematical computer models	
8 Morphology	11-14
8.1 Introduction	
8.2 Optical microscopy	
8.3 Profilometer	
8.4 Confocal	
8.5 Scanning electron microscopy (SEM)	
8.6 Mark depth	

9 Chemical analysis	15-21
9.1 Introduction	
9.2 Theoretical study	
9.3 Energy dispersive X-ray spectroscopy (EDX)	
9.4 X-ray photoelectron spectroscopy (XPS)	
9.5 Attenuated total reflectance single reflection (ATR-SR)	
9.6 Elemental analysis (EA)	
10 Resistance of the mark	22-24
10.1 Introduction	
10.2 Shore hardness	
10.3 Scratch test	
11 Optical characterization	25-28
11.1 Introduction	
11.2 Spectra	
11.3 Color	
12 Conclusion	29-30
13 Future	30
Bibliography (list of related patents included)	

1 INTRODUCTION

A significant effort studying the interaction between light and matter is made because of its chemical, physical and technological interest. Some of the most important processes in nature have the origin in this interaction, like photosynthesis or the sense of view.

Laser is a recently developed technology which gives us the possibility to have a new kind of interaction between light and matter. Laser technology transforms the energy of a source into a coherent (time and space), monochromatic and directional light beam due to the stimulated emission phenomenon. Differences between various light sources are shown in *Figure 1*. The benefits of this technology are shown in several every day products, but they are not always noticeable. Lasers find use in many processes like welding, cutting, marking or surface treatments of different materials including polymers.

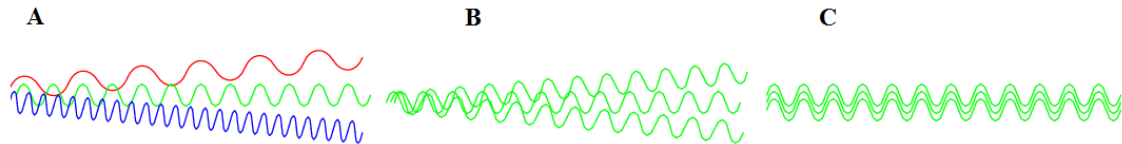


Figure 1: comparison between sun light, led light and laser light [Source: Physicforums.com]

In general polymers are described as macromolecules consisting of a high number of repeating units (derived from monomers) joined by covalent bonds and weaker interactions (hydrogen bonds, van der Waals forces) among the chains. The main components are carbon and hydrogen; therefore polymers are part of the study in organic chemistry. The interaction between laser and polymer is related to the unique characteristics of both and differs for each situation; also considered have to be the effects due to pigments, fillers or any kind of additives usually present in the polymeric materials. Recent years it has been observed how the industry of microelectronics produced a new field of research: *laser ablation of polymers*. The research of laser marking of polymers arises from a similar situation, the technological interest of many industries to customize plastic products and to substitute other technologies like tampography.

2 AIM OF THE WORK

The aim of this work is to develop a methodology that allows future researchers to carry out experiments about the interaction between laser and polymers and facilitate the understanding of results. Due to the lack of applicable studies in literature, information from different sources and fields of work has been collected and tested adapting the experimental methods. The experimental results lead to include or discard these methods in the final Work Methodology. The experiments carried out for the present work cover a wide range of laser wavelengths (355, 532 and 1064 nm) and polymers (results are mostly focused on PP) with the aim to develop a suitable methodology for most of cases. This work is interdisciplinary, with the driving forces being physics, chemistry, materials science and engineering concepts, leading to the collaboration of various groups. Among others the most important groups involved are the group of laser processing of materials and the group of liquid crystals and polymers both members of the University of Zaragoza; and Bosch-Siemens-Hausgeräte (B.S.H.) in Zaragoza and Vitoria.

3 STATE OF ART

3.1 Research articles

The articles about the interaction between laser and polymers are mostly focused on thermal mathematical models and studies about ablation. The purpose of these studies is usually related to microelectronics (1), welding (2-5) or cutting but also found are unsuspected fields like satellite propulsion (6). A brief description of common literature concepts (6-12) is presented below. With this summary the process of ablation can be understood and next chapters are focused in other phenomena less discussed in literature.

Ablation: the removal of material by means of photochemical and/or photothermal laser processes. Ablation is an effect appearing frequently while marking with laser, but is not always necessary and sometimes is not desired.

Incubation: sometimes no visible effects of ablation are noticed after a single or a few laser pulses. A possibility is that the energy is dispersed and does not affect the material. Increasing the number of pulses or changing the frequency of them these effects appear. This phenomenon is called incubation and it has two major causes. The first one is that the material has not enough time to dissipate the energy by mean of phonons; due to this the temperature increases and leads to a thermal process (13). The second one consists in physico-chemical modifications of the bulk. For example changes in crystallinity or bondings. These modifications change light absorption, scattering or mechanical properties for the following pulses. Incubation occurs usually in materials with a low absorption for the applied wavelength. For this work the concept has been related not only to ablation but also to color changes as shown in *Figure 2*.

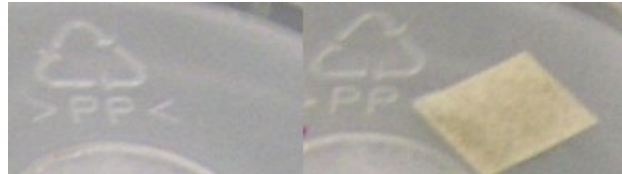


Figure 2: comparison between one and two laser treatment runs on pure polypropylene with 355nm laser, as a macroscopic example of incubation. Mark size is 1x1cm²

Ablation rate: Slope of the ablation curve *depth related to number of pulses* for a fluence value. It is recommended that the incubation period is not considered for the analysis.

Threshold energy fluence: minimum fluence for single pulse ablation. Usually the minimum depth for ablation is calculated to 0.05 μm /pulse. For higher fluencies, depth of ablation increases with fluence until a saturation is reached.

Relaxation time: period of time while the excited state of the polymer persists. A short relaxation time compared with excitation time (considering a two levels system) yields a change of absorption due various effects like bleaching or blocking

Bleaching: in case of one photon absorption conditions the light penetration depth increases due to the saturation of excited states on the surface.

Blocking: in case of multiphoton absorption the opposite effect can occur when in an excited state the surface absorbs all the photons limiting the light penetration depth. In this case due to the excited state the beam is blocked and saturation can be achieved.

Depth (or volume) reached by absorbed energy: it is increased for bad absorbers. Not to be confused with depth (or volume) of eliminated material.

Figures 3 and 4 show experimental results of a 355nm ablation study carried out in this project. The material of the polymer films is PMMA with pigments Disperse Red Aldrich (DR) and Yellow 4.4' Diethoxyazobenzene (DAB) in various contents. Figure 4 shows improved ablation results for PMMA with 2%DR although this film has low value of light absorption for 355nm. This result can be explained because of changes in material properties (e.g. thermal conductivity) that improve the ablation efficiency of the absorbed energy.

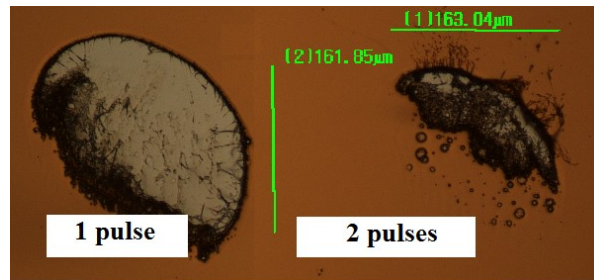


Figure 3: (left) Ablation of PMMA with 2%DR at a fluence value of $1.58 \text{ mJ}/\text{cm}^2$ (right) Ablation is not observed at $0.158 \text{ mJ}/\text{cm}^2$ but after a second pulse the material is affected as shown (incubation). The conclusion is that the threshold fluence is localized between both values.

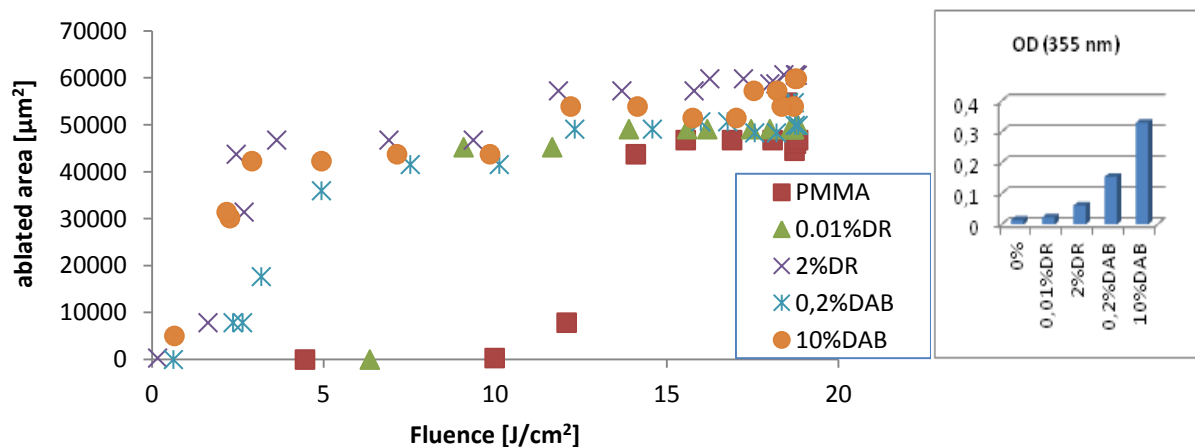


Figure 4: (left) Area of the ablated zone related to fluence for PMMA pure, PMMA with DR and PMMA with DAB. (right) Optical density at 355nm for the studied films.

3.2 Patents

Some interesting patents are listed at the end of this work, most of them owned by various universities and companies like Bosch, Merck or Evonik. The most important concept presented in patents is the use of different components as additives for enhanced laser marking. These are nanopowders consisting of ceramics materials (usually mica) coated with different metallic oxides like TiO_2 . These additives change the absorption and scattering properties increasing the temperature around them. Different combinations of multilayer materials are patented as well. In these products, the layers have different functions; some of them are colored, protective or transparent to the selected laser wavelength.

3.3 Information provided by industries

Information provided by various companies (14-16) offer an overview of the state of art, but information is usually held general. The aim of the texts offered by laser companies is to transmit laser marking advantages compared to, for example, tampography. Advantages are for example quality of mark, time, flexibility, mark resistance, cost, easy and non contact processing, absence of chemical products, precision or textures. Other companies more focused in chemistry offer additives which improve laser marks. A common classification for laser marking phenomena is proposed in *Figure 5* according these texts, these phenomena usually appear combined.

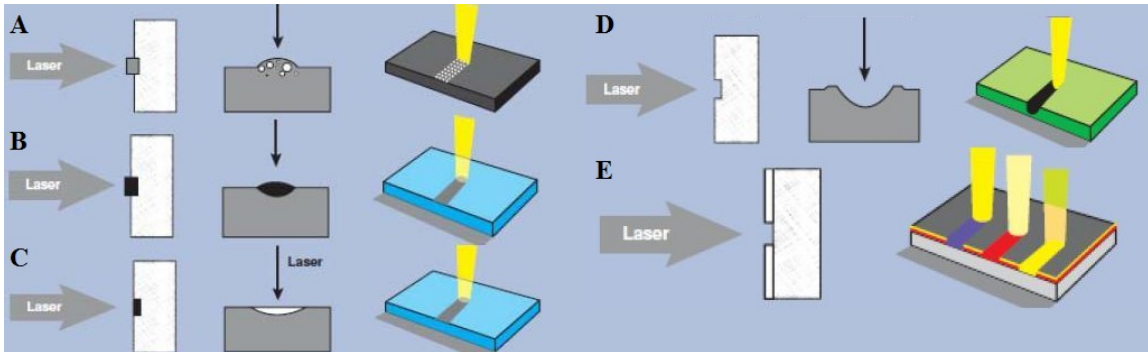


Figure 5: a) Foaming b) carbonization c) photoreduction of TiO_2 d) engraving e) ablation of multilayer material [Source: DSM engineering plastics]

Foaming: by means of a pyrolysis reaction small quantities of gas are generated. The gas produces a light or white colored foaming and as a result a curved surface is observed. This process can be enhanced by some additives like carbon black (18).

Carbonization: material is thermally decomposed due to high pulse intensity. As a result a dark color is produced (17).

Photochemical processes: Zheng H.Y. (19) proposed a change in oxidation state of bipyridilium obtaining green and red colors. The most cited chemical process (14-17) is the photo reduction of TiO_2 (a.k.a. cold marking). It appears frequently because of its use in white pigments or stabilizers. Among others, this oxide is also used as wavelength absorbant in transparent materials, increasing the temperature around and producing bubbles or microcracks.

Engraving: the material absorbs high quantities of laser energy cutting the material surface, producing damages and low color contrast. This process is frequently used for marking industrial information on products (e.g. bar codes) but they do not have an aesthetic purpose.

Ablation marking: selective photochemical or photothermal removal of superficial layers on a multilayer material resulting in multicolor marks. It offers better accuracy (e.g. edges or corners) than engraving. In automobile industry ‘*Night and day*’ marking is used for many buttons. It consists in translucent polymers painted or coated, this coating is partially removed drawing different symbols and those are illuminated with color leds.

Chromophore destruction: by means of photochemical and/or photothermal processes some bondings can be broken. If the chromophore molecules are destroyed it produces a color change.

Among others, depending in laser wavelength some lasers are more connected with some effects than others (*Table 1*)

Table 1: laser wavelengths and related phenomena [Source: web of DSM engineering plastics]

Wavelength	Phenomena		
CO2 (Far IR)	Engraving		
Near IR	Carbonization	Foaming	Thin layer ablation
Green	Carbonization	Foaming	Thin layer ablation
UV	Cold marking without thermal interaction		

The process is also dependent on the polymer types and additives (*Table 2*):

- Markable polymers without additives [Source: Trumpf lasers]:

ABS, PC, PPSU, PBT, SAN(styrol), UREA, PEEK.

- Markable polymers with additives [Source: Trumpf lasers]:

PS, PE, PI, PA, PETP, PVC, POM, Polyester, PPS, PU, ASA, Polyolefine (PEHD, PP), PES, PMMA, PEI, PTFE.

Table 2: effects of various additives [Source: web of DSM engineering plastics]

Phenomena	Organic pigments	Inorganic pigments	Glass fibres	Minerals	Carbon fibres	Flame retardants	Laser additives
Carbonization	No	+	No	-	+	+	+
Foaming	No	+	No	+	-	-	

4 PHOTOCHEMICAL AND PHOTOTHERMAL PROCESSES

Literature classifies the interaction between laser and polymer into three categories (8,11,20). Photothermal processes (20,21) involve multiphoton absorption, increase of temperature, fusion, evaporation,. In photochemical processes (9) just one or two photons are needed to break certain chemical bondings; for example, a (C-C) bonding has a cohesive energy of 3.6eV similar to 3.5ev (355nm photon). But these are just ideal conditions and actually must be observed that processes remain between the mentioned limits and are called photophysical processes that also include stress waves (22), fragmentation and ejection of material particles. The term photochemical or photothermal is used when an interaction tends to one on them. Nowadays it is easier to achieve thermal processes because of the simple nature of this interaction and the high development of IR lasers. Daniel Sola (23) considered the excitation process time (t_R) and thermalization (relaxation time of excitation process) of excitation energy (t_T):

Photothermal: $t_T \ll t_R$ The laser is a heat source localized in time and space.

Photochemical: $t_R \ll t_T$ The system temperature under laser irradiation is invariable.

Feng Y. (24) developed a ratio of the rates of photochemical reaction related to heat-driven reaction during laser polymer ablation via a 248-nm excimer laser on PP. For a single pulse the graphic dependent of fluence and ratio Ra is shown in *Figure 6*.

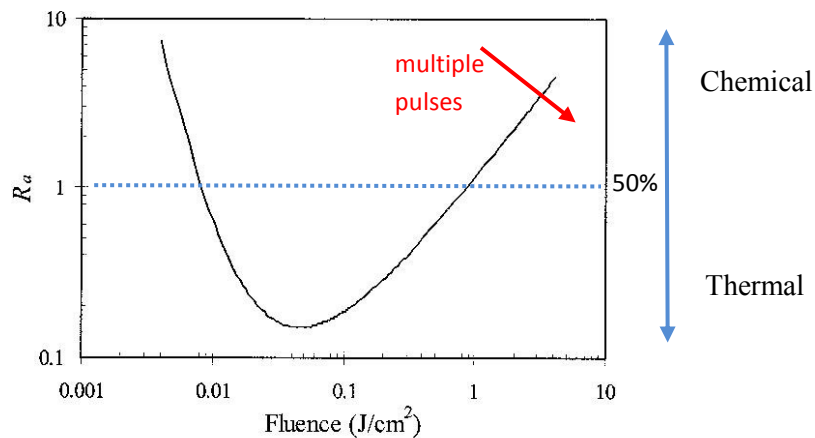


Figure 6: $Ra=1$ is a ratio 50% chemical and 50% thermal, over this point (1-10) the process enhance the photochemical proportion. Fluence is provided in the horizontal axis.

For multiple pulses the right side comes down and higher fluence is necessary to reach $Ra=1$ and pass to photochemical processes in this side of the graphic. During laser polymer marking the situation is more similar to multiple pulses.

The literature (6,9) offers other parameter tendencies. Short wavelength, short pulse time and high irradiance leads to photochemical processes. Also a material with a high absorption coefficient, low thermal conductivity and low absorption depth leads to the same situation. Others phenomena like plasma generation, the atmosphere, energy distribution during a pulse, frequency or the materials temperature can affect the type of process.

5 DESIGN OF EXPERIMENTS (DoE)

In the study of laser marking of polymers a large number of parameters has to be considered, each one with its own range of values; thousands of combinations are then possible and it increases the time of work if the researcher does not properly design its experiments. For the present work the marks have been produced combining pairs of selected laser parameters (*Table 5*); the matrix distribution allows fast viewing and comparison (*Figure 7*). It is recommended to reduce the number of experiments according to a fractional factorial design and at the same time selecting the most representative marks for each explained phenomenon.

Table 5: laser parameters (*d* is focal length)

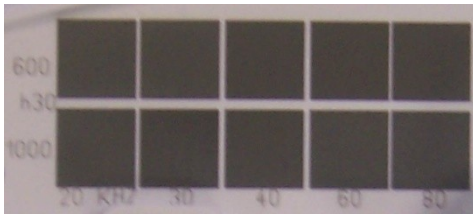
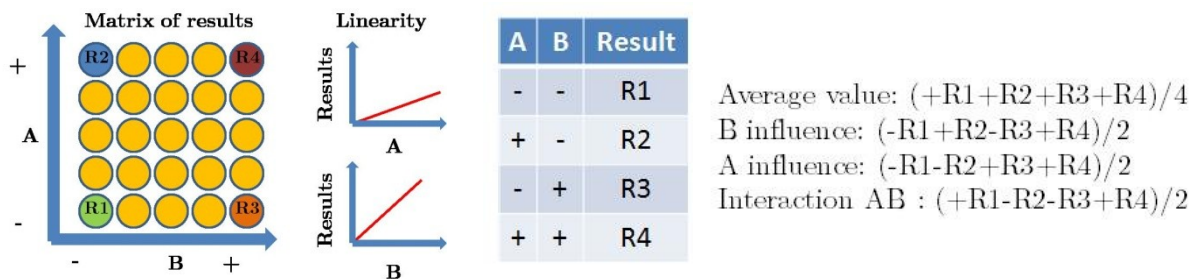


Figure 7: matrix of laser marks in ABS

Name	Symbol	Usual units
Frecuency	f	kHz
Distance between lines	h	µm or nm
Velocity	v	mm/s
Distance lens-sample*	d±x	mm
Wavelength	λ	nm
Pump power	Pp	A or %

A factorial fractional design (25,26) allows to determine the effect of each parameter and their interactions. This mathematical process, whose easiest situation is explained in *Figure 8*, assumes a linear evolution of results; otherwise linearity can be emulated by a piecewise linear function. The factorial condition allows discard interactions of more than three parameters.



FACTORIAL DESIGN 2 ²				
Levels	A frequency [kHz]		B velocity [mm/s]	
	+	-	+	-
	80	20	3000	600
A	B	Roughness [µm]	Average roughness 6,8665	
-	-	9,7	Effect	
+	-	7,585	f	1,583
-	+	2,45	v	-3,552
+	+	7,731	f x v	3,698



Figure 8: (up) 2² factorial design step by step (down) It is a real example of UV (355nm) laser marking of black PP, the high effect of f x v interaction allows to discard the single parameter influence. Roughness is mainly affected by the difference between the values of f and v

6 PREPARATION OF SAMPLES

6.1 Introduction

Material samples have to be obtained and marked; for this work the standard marking size is $1 \times 1 \text{ cm}^2$. It is desirable to have a personalized selection of raw material, pigments, additives and its mixture. On the other hand without the possibility to personally produce the samples, the chemical content of the bulk has to be studied as will be described in *Chapter 9*.

6.2 Polymer films

These kinds of samples are used for the ablation studies described in *Chapter 5*. It consists of a thin film coated on glass substrate. For example the thin films of PMMA shown in *Figure 9* have been generated with a spin coater and an ozone generator (glass surface activator). PMMA has been previously diluted in cyclopentanone and pigmented. As mentioned, these samples shown efficacy for ablation studies but are not useful for multiple larger laser marks matrix. Obtaining the samples and marking it one by one enlarge the cycle time. Furthermore the glass can interact with the film altering temperature distribution, shifting the polymer deformation near the interface or transmitting shock waves.

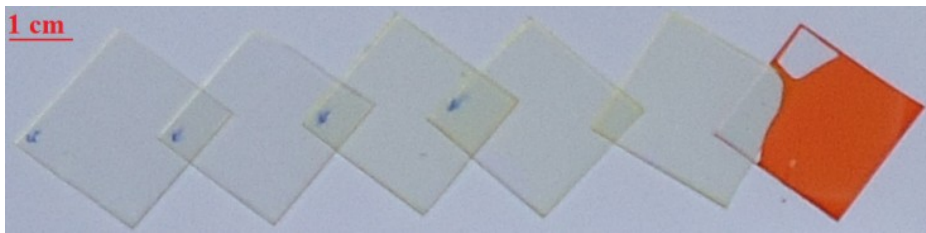


Figure 9: various PMMA thin films on laboratory glass

6.3 Bulk

Obtaining larger and wider samples is possible due to other devices as extruders, injection or press molding. The advantages are extensive surface and thickness and no need of substrates. An extensive surface is needed to produce multiple marks at once, distributed as a matrix. A laboratory press molding device has been tested; this device is useful to generate a low number of samples. The cycle time is of 2h for the sample in *Figure 10* and previously the material has to be pulverized and properly mixed with the additives.

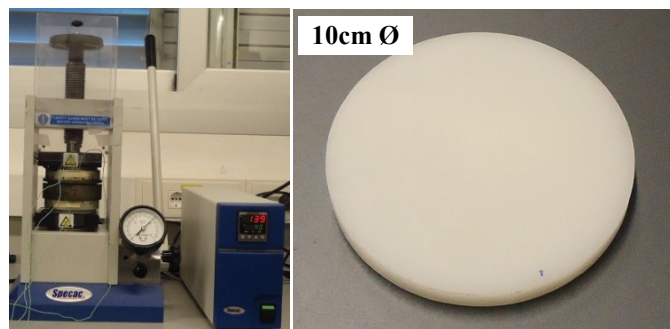


Figure 10: (left) Press molding device, max. $T=300^{\circ}\text{C}$, max. load 10T (right) PET sample

Also an injection molding machine has been tested, more samples per time unit can be produced. Two molds, for flat and large surface bulk samples ($100 \times 100 \times 3 \text{ mm}^3$, $50 \times 50 \times 3 \text{ mm}^3$), have been modeled using specialized software (*MoldFlow*). Also two positions for the injection point have been tested, these two positions are located at the center of the square and the center of a square side (*Figure 11*). Lightly more homogeneous results in temperature, pressure and shear have been obtained with the injection point at the center of the square. *Figure 11* is representative for the simulated polymers of *Table 4*.

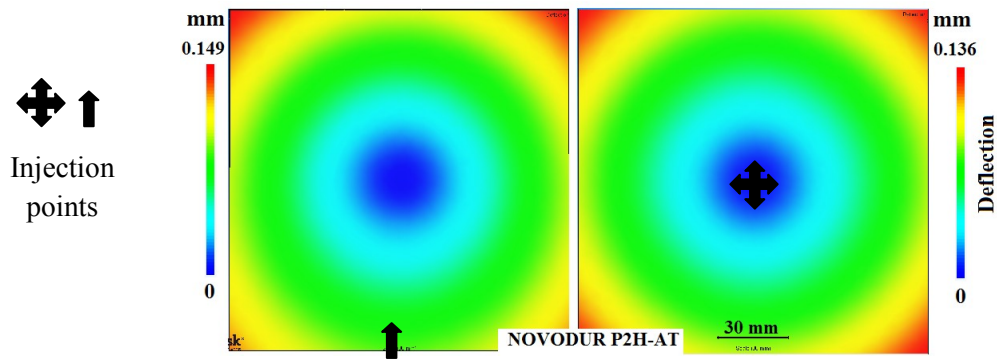


Figure 11: simulation of deflection for injected Novodur $100 \times 100 \times 3 \text{ mm}^3$ sample

Table 4: materials simulated for injection process

Material	Code and povider	Comments
PP	620/2 SV51734 MCO (Alcom/albis)	Silver PP homopolymer.
	575 P (Sabic)	PP homopolymer.
	RA 12 MN (Sabic)	PP random copolymer.
	Hostacom M1 U13 Natural (Basell)	10% mineral filled PP homopolymer. (PPTV10)
	Hostacom M2 U01 Natural (Basell)	20% mineral filled PP homopolymer. (PPTV20)
PBT/PET	Valox® 830 (GE plastics)	30% glass fibre reinforced PBT+PET blend.
SAN	LURAN 368 (BASF)	
ABS	Novodur® (Bayer)	

Unusually laser marks show defects depending on injection conditions. It happens due to stresses or a deficient mixture with the pigment combined with non aggressive laser processes (low fluence or low absorption). *Figure 12* shows microcracks in marked purple SAN whose direction depends on the position around the injection point; the second image shows inhomogeneities in marked black PP.

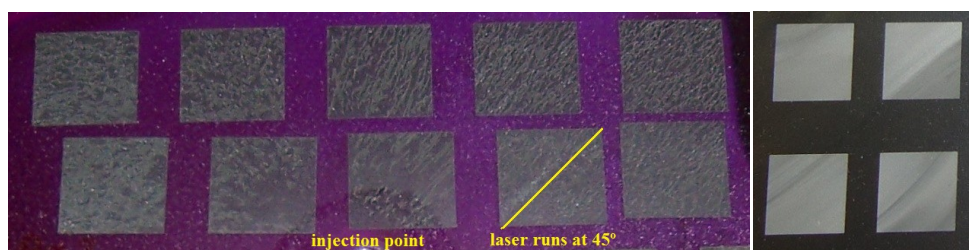


Figure 12: (left) Laser marks with directional microcracks in SAN (right) Inhomogeneity in PP

7 TEMPERATURE

7.1 Introduction

The different phenomena appeared while marking are temperature dependent; for example lower temperatures are expected for photochemical processes. When having a wide zone with stable temperature during all the process then it is possible to have an approximation of the temperature by means of pyrometers, thermocouples or thermal cameras.

7.2 Pyrometer

This non contact device measures temperature supported on that IR energy is proportional to the 4th power of object temperature. Opaque organic materials have an emissivity value around 0.95 near to the ideal black radiator value 1. The emissivity of a material changes if there are variations in temperature or color. Shaochen Chen and Costas P. Grigoropoulos (52) designed a specific pyrometer for Ni-P disks temperature measurement with nanosecond-time-resolution but even in this case the measurement area was 5.5 mm x 1.5 mm wide. A commercial pyrometer has been tested for this work (Figure 13).

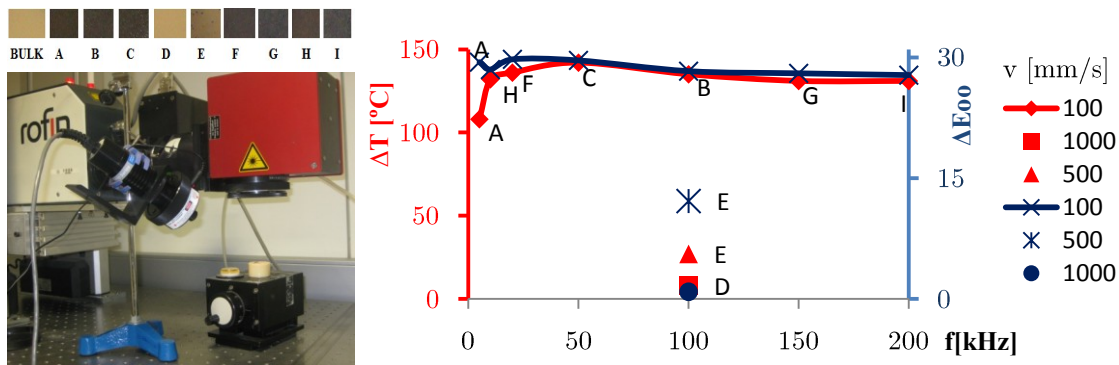


Figure 13: (left) Pyrometer disposition for temperature measurement and photography of various marks on PBT (right) Temperature increase and color distance related to frequency for the same marks.

With the tested pyrometer the temperature of a zone with a size of (minimum) 12.5 mm² is interpolated. Consequently the measured temperature is not the spot area value but an average value of a larger zone. Moreover it has high response time (0.5s) and a non accurate positioning of the pyrometer produces high value dispersion; in this case dispersion about $\sim 50^{\circ}\text{C}$ was observed varying the position of the pyrometer 1cm. The results achieved marking PBT are shown in Figure 15. This graphic shows a relation between color distance ΔE_{00} (will be explained in Chapter 11) and increase of temperature. In this case the dark color is related to carbonization.

7.3 Mathematical computer models

Due to the complexity of the temperature measurement handling traditional methods, a second possibility is proposed. Mathematical computer models are common in literature (4,5,8,27-30) mostly for single pulse thermal ablation processes. B. Sinkovics et al (31) reviews different ablation mathematical models and creates an improved one. No specific models have been found for laser marking as many processes can occur and the contribution of each is not specified.

8 MORPHOLOGY

8.1 Introduction

With the aim of understanding the interaction between laser and polymer a close viewing of the surface is required (32). Each possible phenomenon shows distinctive textures and cross section profiles as seen in *Chapter 5, Figure 5*. A choice of devices for surface analysis has been tested and the results are presented below. The studied materials are mainly black (2% weight of pigment) and white (5% weight of pigment carbon black) polypropylene homopolymer with 10% weight of talc, from now coded as black bulk and white bulk respectively.

8.2 Optical microscopy

The most basic tool for close surface inspection is based on optical lenses. This technology allows fast imaging (*Figure 14*) but does not provide roughness values or profiles. An optical microscopy is usually included in other devices that are explained in this Chapter.

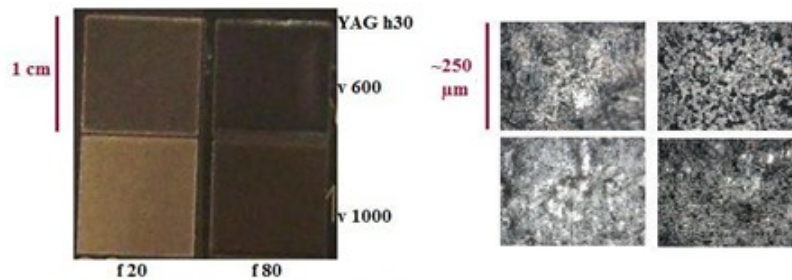


Figure 14: images at two different scales of black ABS marked with 1064nm laser

8.3 Profilometer

A profilometer allows the acquisition of quantitative information (e.g. roughness, peaks height) about a profile. As experimental comparison, after five measurements of a PBT film height the average result ($3 \pm 0.09 \mu\text{m}$) was $0.005 \mu\text{m}$ higher measuring with a contact profilometer than using confocal. With this result both devices demonstrate to provide similar information on studying profiles. Profilometer shows a disadvantage analyzing extensive marks with non homogeneous texture because not all profiles are representative and multiple profiles are needed.

8.4 Confocal

Confocal microscopy is an optical imaging technique with improved features which enables the reconstruction of 3D surface structure from the obtained images by using point illumination and a spatial pinhole. In the course of confocal studies for the present work it has provided full information about 3D imaging, roughness or profiles and a main question arises: the handled confocal allows diverse lens between 10X and 50X and also the size of the studied zone has to be defined. For a high number of studies these decisions (lens and size) significantly affect work time and a bad selection can lead to non representative results. 50X objectives offer better accuracy, but at the cost of smaller studied areas or higher working times. Side-to-side rectangular

3D images are representative of the entire surface and allow complete profiles. *Figure 15* shows a complete confocal study for two marks of black bulk.

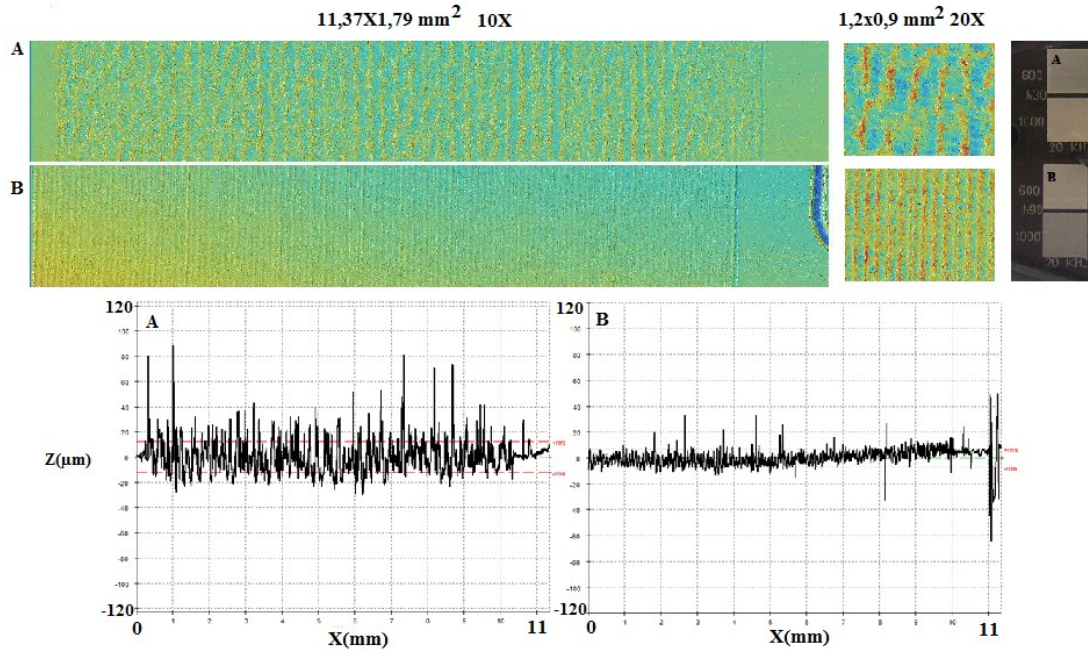


Figure 15: confocal analysis of two laser (355nm) marks of black bulk at 600mm/s and 20kHz. A, B are marked respectively with 30 and 90µm between lines. The figure includes side-to-side 10X image and profiles, 20X detail and photography. The grooves indicate engraving.

The profile can be explained according to the possible phenomena: it is expected that elevated profiles appear for foaming (higher) or carbonization (lower), absence of material for ablation, grooves for engraving and the surface height remains in the case of pure pigment chemical destruction. Two examples are shown in *Figure 16*.

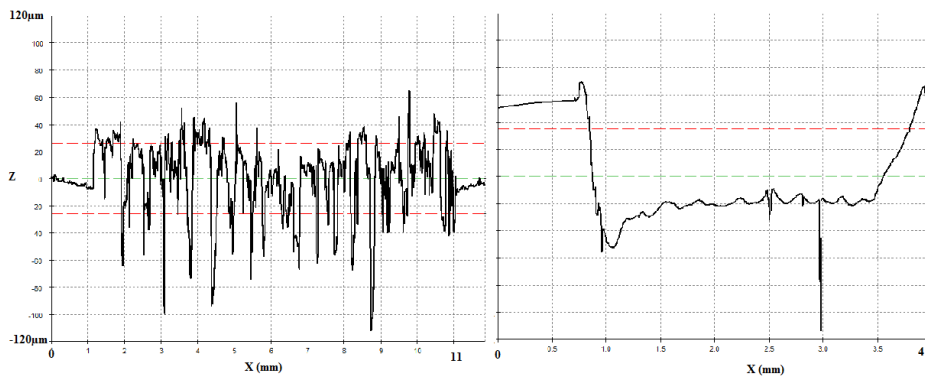


Figure 16: (left) foaming in pure PP after (right) engraving on black PBT

Confocal allows direct roughness measurement in wide areas. 10x lens offers an adequate measurement of surface roughness for viewing its graphical evolution related to various parameters (*Figure 17*). The graphic shows minimum roughness at higher velocities, it is explained because of larger distances between laser pulses producing a surface texture more similar to the original bulk (~3 µm).

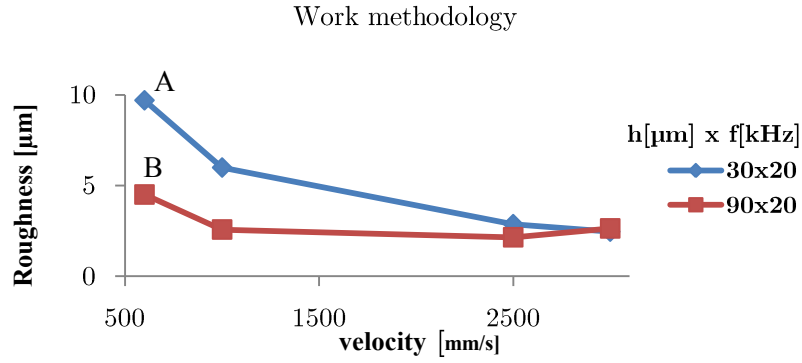


Figure 17: average roughness for various laser marks at 10X including marks A,B of Figure 15.

8.5 Scanning electron microscopy (SEM)

Scanning the surface by means of a high energy beam of electrons produces various signals depending on the interaction with the atoms of the sample. If backscattered electrons are analyzed, it allows representing atomic weight, dark colors indicate light elements and vice versa. If secondary electrons are analyzed then morphology is observed with high accuracy (details size less than 1nm). Moreover, the same instrument can realize EDX analysis; this technique will be explained in *Chapter 9*. SEM offer more accuracy than other proposed devices but is also more complex. *Figure 18* shows black bulk marked with 1064 nm wavelength laser.

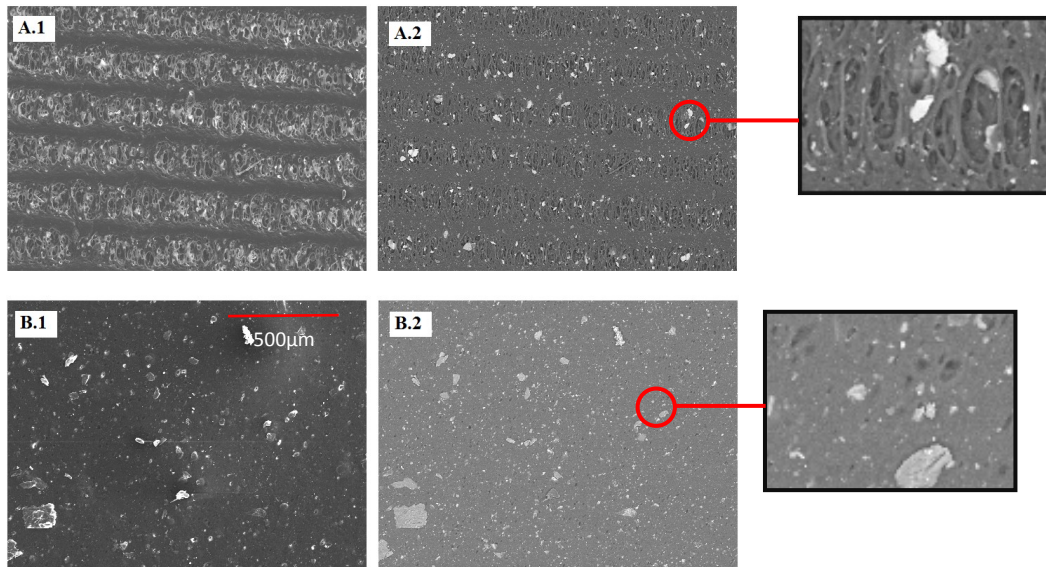


Figure 18: black bulk marked with 1064 nm laser. A.1 and A.2 marked at 3000 mm/s, 20 kHz and 30 nm between lines. A.1 secondary electrons, A.2 backscattered electrons. B.1 and B.2 marked at 3000 mm/s, 80 kHz and 30 nm between lines. B.1 secondary electrons, B.2 backscattered electrons

Backscattered electrons allows the identification of numerous particles heavier than the rest of the material in *Figure 18*. The zoom of A.2 image shows signals (e.g. crater, deformed material, strings) of photothermal interaction and/or gas generation. Images B.1 and B.2 do not seem to be affected but compared with bulk image of *Figure 19* some changes as a new texture, smaller pores and some bigger particles are detected. Confocal images and photographs of the marks are included in *Figure 20*.

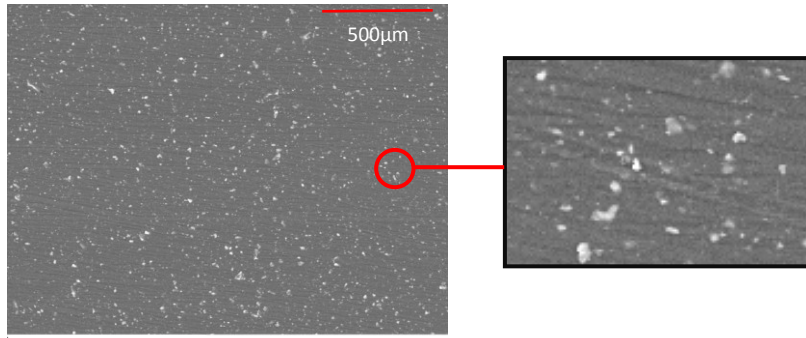


Figure 15: black bulk backscattered electrons image, injection marks are present due to mold texture. No pores are observed. The particles have smaller size than in laser affected zones.



Figure 26: photograph of marks A and B of Figure 18, each mark size is $1 \times 1 \text{ cm}^2$. Confocal images size is $1.2 \times 1 \text{ mm}^2$

8.6 Mark depth

Besides surface information also the penetration of the laser beam affecting the material can be measured. Sometimes (e.g. SAN) the mechanical properties allow a brittle fracture along the mark. Cutting and/or polishing a mark section produces plastic deformation in several polymer materials, in these situations cooling below glass transition temperature allows a brittle fracture without deformation. Structural or color changes determine the mark depth with the same instruments previously explained. Figure 21 shows an example of SEM measurement.

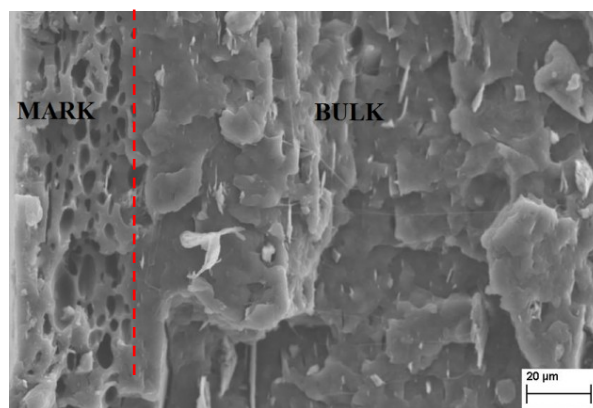


Figure 21: secondary electrons image of the mark B of Figure 15(SEM). The affected zone contains numerous cavities due to the generation of gas. Mark depth is around $40 \mu\text{m}$.

9 CHEMICAL ANALYSIS

9.1 Introduction

There are two main reasons for chemical studies of marks and bulk. The first reason arises from *Chapter 6* when it was explained how to obtain the bulk samples. One possibility is to work with commercial polymeric samples with a deficient knowledge about the type and percentages of additives as the suppliers tend to protect the formulations. Information about the type of additives used depending on the type of polymer can be found in additives handbooks (33,36) or specific literature articles (37,38). This reason leads to recommend having always the greatest possible control during sample preparation (*Figure 22*). The second reason for chemical studies is to understand which kind of chemical processes appear while marking. Information about chemical composition and structure of the bulk samples and after marking provides information about elements removed or chemical processes on marking. Even controlling the generation of bulk samples it is possible to find unexpected contents or known just the commercial code of an additive, also a previous theoretical and experimental study of the raw material, additives and colorants is recommended.

In order to find out the chemical microstructure of polymers spectroscopic techniques like NMR (33), IR and Raman (32) are commonly used (21). Surface analysis can include XPS (11,17), SIMS, SEM (11), TEM or AFM. Analysis of gases (34,35) or ejection of particles (9,32) can also be achieved. All these studies can normally be applied to bulk as any other polymer but the special characteristics of the mark (thin layer on the surface) make its study more complicated.

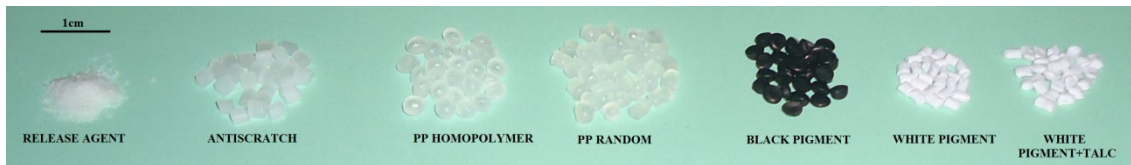


Figure 22: various raw material, additives and pigments.

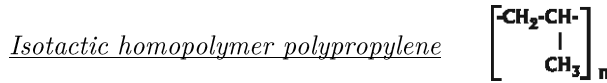
9.2 Theoretical study

The first step is to find the polymer formula and its properties in a polymer handbook (33). Thermal properties are related to thermal decomposition (21,53) that is described in safety guides because of its potential toxicity. The second step consists in finding information about common additives and to deduce possible contents according to the color of the material (*Table 5*). For example carbon is expected in black polymers and titanium and/or zinc in white polymers. A full example about PP according to the cited references is also presented:

Table 5: elements that usually appear in some pigments. Toxic elements as Pb or Cd are replaced with new formulas in Europe.

Pigment color	Black	White	Red	Green	Blue	Yellow
Possible content	C, Ti	Pb, Ti, Ba Sb, Zn, S	Cd, Fe, Pb, Hg	As, Cd Cr, Cu	Co, Cu	Cd, Cr, Zn Co, Ni, Ti

Work methodology



Temperatures: melting 460.7K glass transition 270K decomposition 473K

Density [mg/m³] at 298.2K: crystalline 0.93-0.94 amorphous 0.85

Cristallinity by X-ray (%): for injection molding 61-62

Isotactic index: for injection molding >0.95

Water absorption after 24h immersion (%): for injection molding 0.03

Common stabilizers and antioxidants: phenols, amines, sulphur-compounds, calcium stearate.

Fillers and pigments: carbon black, TiO₂, hydrated chromium oxide, glass fibre (max. 30%).

Antistatic: ammonium salts, glycolic ester.

Products emitted during decomposition: Hydrocarbons C₂-C₁₂ (mostly saturated). Acetone and methylethylketone. Formaldehyde, acetaldehyde, acrolein. Acetic and crotonic acids. Carbon dioxide. Gases and other volatile products due to additive decomposition and volatilization.

Theoretical content for a common PP compound is shown in *Figure 23*.

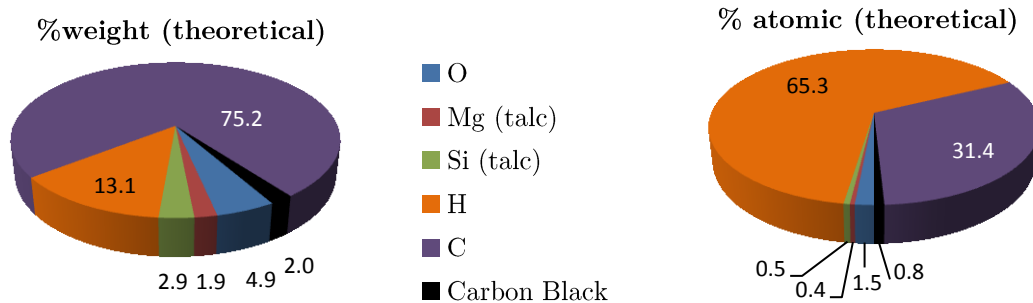


Figure 23: weight and atomic percents for black bulk.

9.3 Energy dispersive X-Ray spectroscopy (EDX)

SEM has been described on *Chapter 8* with morphological purposes; the same device allows EDX analysis. In an electronic microscope, an electron beam reach the sample. The interaction between the electronic beam and the material produces various signals including emission of X-rays. This signal is related with the chemical content of the material. A disadvantage of EDX is that an electrical conductor coating is needed for insulating samples. For the present work the experimental analysis of EDX has been made using a carbon coating. EDX cannot quantify hydrogen content and (due to the coating) neither carbon has been quantified. Furthermore, EDX has low accuracy in analyzing elements present in small percentages. An example (*Figure 24*) is proposed consisting in a sample of black bulk marked with 1064nm wavelength laser. With EDX graphics of *Figure 24* no conclusions have been obtained, the variations are in the order of the device sensibility (around 1%). When various graphics about percentage are compared it can be observed that a variation in percentage is not always related with the same variation in real content. For example an increase in Si and Mg atomic percent after marking, as any source of both materials is present, would be interpreted as a decrease of real content of other elements. The graphics have been made studying extended zones, also an analysis of particular points has been made and Ca, Na, S, Cl, Al, K, Fe and N have been detected. The quantification of these elements is not possible and it is difficult to know if the selected points are representative.

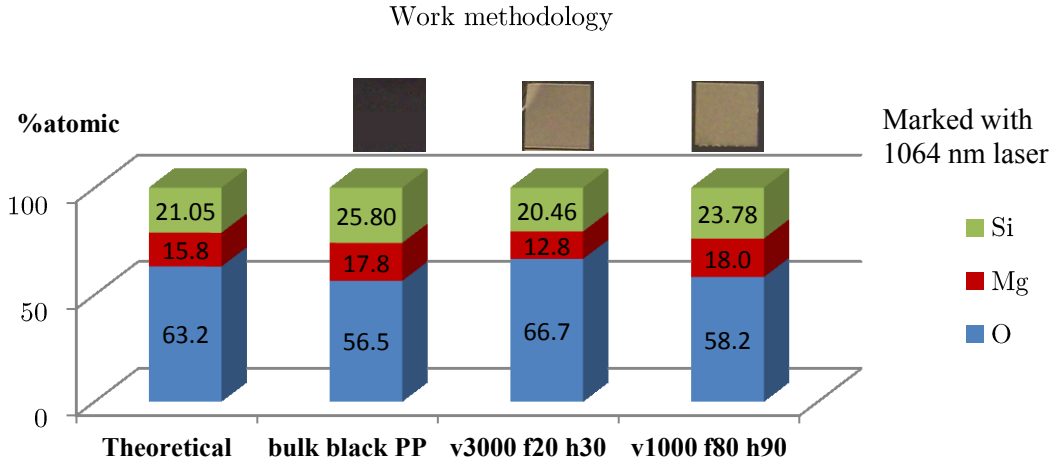


Figure 24: (left to right) Theoretical result expected in a EDX analysis for black bulk. Real result for bulk and results for two areas marked with different laser parameters: v [mm/s], f [kHz] and h [μ m] between lines. Photographs of the bulk and marks are included.

9.4 X-ray Photoelectron Spectroscopy (XPS)

With XPS the sample is exposed to a X-ray beam, the surface emits photoelectrons that are detected and translated into information about elemental content and its bondings. XPS technology works in atomic percent and allows detection until $\sim 0.1\%$ atomic (He and H cannot be detected) with an accuracy about 5-10%. The main difference with EDX is that XPS collect information just in the outer-most layers of the sample (3-10 nm). The studied area is in a range from 15 to 1000 μ m (diameter), the standard for this work is 700x300 μ m². An important characteristic is that XPS allows identifying chemical bondings performing an ‘in depth’ study.

A white bulk study is proposed in Figure 25, it has been marked with 355nm and 532nm wavelengths lasers using with various parameter combinations: frequencies 60 and 80 kHz, velocities between 600 and 3000 mm/s and 30 μ m between lines. The absence of magnesium can be related to diffusion phenomena, device accuracy (5-10%) or to a non homogeneous mixture.

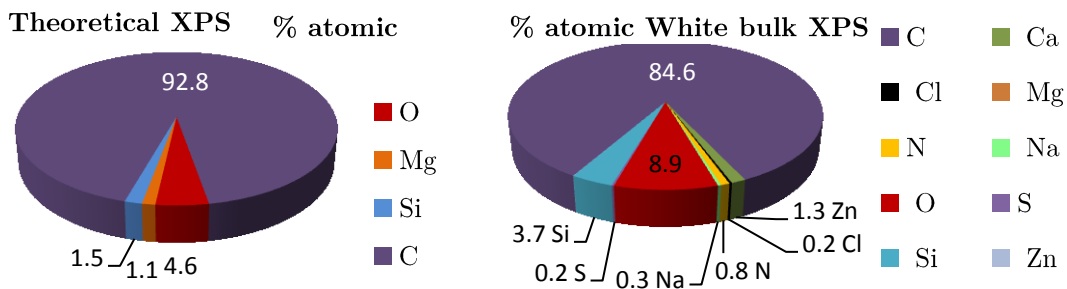


Figure 25: theoretical (H excluded) and real result for white bulk XPS study. The 5% of white pigment is not included in the theoretical graphic.

Interesting changes are observed after the laser marking, similar results are found for 355 nm and 532 nm wavelength lasers. Figure 26 is representative of these results.

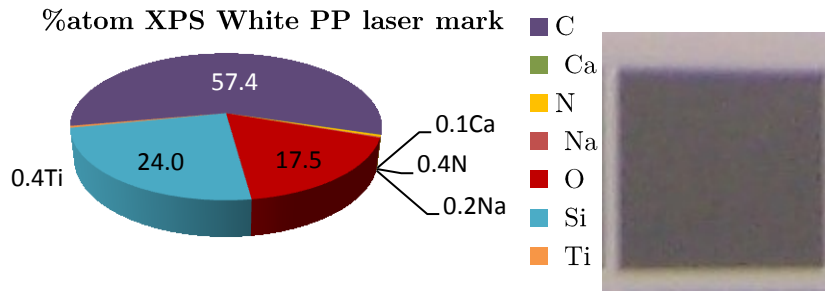


Figure 26: white bulk marked with 355nm laser at 2500 mm/s, 60 kHz and 30 μ m between lines

An increase in oxygen and silicon atomic percent and also a decrease in carbon atomic percent is observed. A real increase of silicon content is not expected upon marking as there is not any source of silicon. An increase of oxygen content is possible (air) but comparing silicon and oxygen percentage variations this option can be discarded. A decrease in carbon content is possible and can explain the graphic. Also has to be considered interactions with hydrogen, whose content is unknown. The information collected in the theoretical study of Chapter 9.2 indicates that generation of organic gases containing carbon is expected and it is agree with the result. This process is possibly affecting to the white pigment by losing its coloring skill.

Until this point marks have been always compared with bulk but another interesting source of information is the comparison between marks related to the evolution of a laser parameter. *Figure 27* shows the evolution of atomic percent of the most abundant elements found in white bulk related to laser marking velocity. The decrease of carbon percent is related to an increase in velocity and it is also related with a decrease in fluence (energy/area). Lower fluences could be improving the photochemical rate enhancing the removal of carbon atoms (producing hydrocarbons) without increase of temperature.

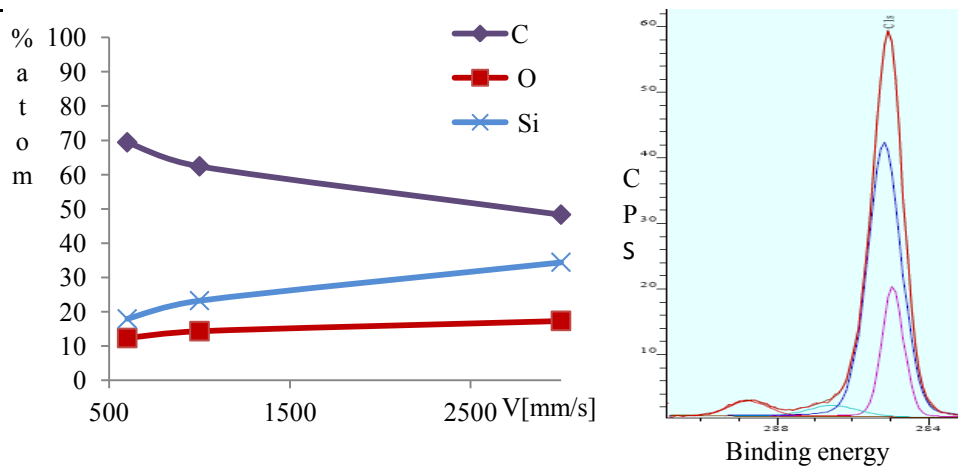


Figure 27: (left) Evolution of C, Si and O percent for white bulk related to velocity. Other laser parameters are 355nm, 60kHz and 30 μ m between lines (right) C1s curve deconvolution example

Finally an ‘in depth’ study for determining element bondings can be developed by curve deconvolution (*Figure 27*). For example, low (or none) quantities of Ti have been observed in white bulk but when it has been found in a marked area two types of titanium oxide appear. It is explained as photoreduction of TiO₂ to TiO. The chemical environments for each atom are iden-

tified according to literature, it is noted that peaks can be displaced toward right because of an increase in material electric charge due to the interaction between X-rays and electrons. A full example for carbon and oxygen is shown in *Table 6*.

Table 6: comparison of C1s and O1s deconvolution for white bulk, 355nm laser mark at 2500mm/s and 532nm laser mark at 3000mm/s. Both marks at 80kHz and 30 μm between lines.

C1s	White bulk				355nm mark				532nm mark	
Bonding energy	284.94	286.53	288.74	285.16	284.98	286.51	288.67	285.64	285.03	285.53
Curve area %	21.08	4.1	4.67	70.15	87.24	5.31	2.8	4.65	73.33	26.67
O1s	White bulk				355nm mark				532nm mark	
Bonding energy	532.09	533.98			532.47	531.28	533.02		532.72	533.42
Curve area %	96.95	3.05			72.46	9.56	17.97		66.2	33.8

Rough conclusions about carbon and oxygen deconvolution are achieved; the peaks can be related to various bondings (e.g. 285eV to C-H or C-C) and they are probably displaced toward right. The results seem to be according with a PP structure of hydrocarbons (most percentage around 285eV) that remains after marking. It seems to be achieved a decrease in the carbonyl group (288eV C=O) that could be related to the removal of an additive, this result is supported by the ATR analysis explained in the point 9.5. A general explanation of the results can be the removal of organic compound keeping the inorganic by oxidation.

A complete XPS analysis has been also realized on black bulk (*Table 7*), the deconvolution results are not exposed because rough conclusions are achieved again. This XPS study shows lower variations (bulk-mark) of atomic percents than the ones in white bulk; furthermore it is observed the same absence of Mg. The generation of organic gases containing carbon explains the decrease of carbon and oxidation the increases of oxygen; it fits with the phenomenon of foaming. The lower percentage variations compared with white bulk can be explained because of an increase of the photothermal rate that remove not only C, O and (probably) H but also is more aggressive for the rest of elements that are removed in a similar proportion. It has been used the same laser parameters for white and black bulk when marking with 532 nm, so the difference of results is attached to the color and/or the elementary content of the pigment. This difference of results is also supported in the ATR study explained below.

Table 7: atomic percent XPS analysis of black bulk and marks. Laser parameters are 80kHz and 30μm between lines; wavelength [nm] and velocity [mm/s] are shown in the table.

Sample	Al	C	Ca	Cl	K	Mg	N	Na	O	S	Si	Zn
λ[nm]/v[mm/s]	2p	1s	2p	2p	2s	1s	1s	1s	1s	2p	2p	2p
Black bulk	---	89.3	0.4	0.2	---	---	0.6	0.1	5.5	0.1	3.7	---
532/600	0.3	82	0.6	0.4	0.3	0.1	1.4	0.5	10	0.5	3.7	0.14
532/1000	---	86.2	0.8	0.3	0.3	---	0.9	0.4	8.3	0.5	2.4	0.04
532/3000	---	85.6	0.5	0.3	---	---	1.1	0.5	9.3	0.3	2.5	0.03
1064/3000	0.2	78.8	0.2	0.5	0.2	---	2	0.8	13	0.5	3.9	0.02



9.5 Attenuated total reflectance single reflection (ATR-SR)

ATR is an IR sampling technique; it allows characterization, identification and also quantification of many substances. ATR measures the changes occurring in a totally internally reflected IR beam when it comes into contact with a sample (*Figure 28*). The IR beam is addressed with a certain angle onto a crystal with a high refraction index. It creates an evanescent wave that protrudes 0.5-5 μm beyond the crystal surface and into the sample. The evanescent wave is attenuated or altered by the absorption of energy on the sample surface.

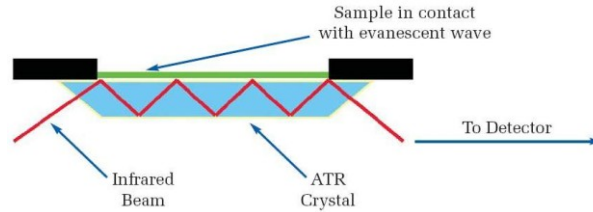


Figure 28: ATR schema [Source: www.perkinelmer.com]

Black and white bulk and two marks are proposed as examples for ATR analysis in *Figure 29*, the researcher has to identify the characteristic polymer peaks and peaks that belong to additives or pigments. IR spectra of white and black bulk are similar and not important differences related to the additive bands are observed. The main peaks belong to the polymeric chain:

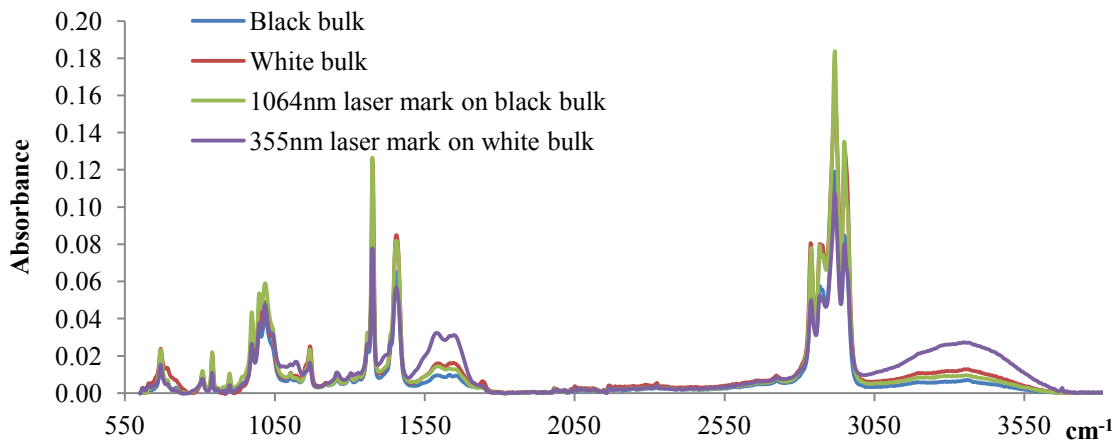


Figure 29: ATR analysis for black and white bulk and two laser marks.

2800-3000 cm^{-1} : 4 peaks related to stretching of C-H bonds of the olefinic macromolecules.

1450-1475 cm^{-1} : these peaks corresponding to methyl asymmetric deformation CH_3 and methylene deformation vibrations CH_2 , mainly the last one.

1375 cm^{-1} : characteristic peak of PP, related to the symmetric deformation of CH_3 .

700-1200 cm^{-1} : in this zone various peaks are found, they correspond to macromolecule skeletal vibrations. Specifically three typical peaks between 800 and 900 cm^{-1} appear; also around 900 cm^{-1} two peaks were expected but three are observed, the third one is possibly due to an additive.

The peaks above reported are ascribed to polypropylene but the most difficult part is to find, discuss and conclude about the rest of peaks. Three main 'unknown' peaks appear around 1600cm^{-1} , 1750cm^{-1} and 3300cm^{-1} (this one is a wide zone). Those peaks could be related to thermal stabilizers like phenolic compounds, for example Irganox 1010 or similar. This type of compounds presents peaks corresponding to: aromatic (1600cm^{-1}), ester (1750cm^{-1}) and OH (3300cm^{-1}); but this relation of peak intensities was not expected for Irganox 1010, a more intense peak for ester and a less intense peak for OH would be more appropriate for Irganox 1010. Finally it is concluded that other phenolic compound, a mixture of various including Irganox or a mixture with other type of additives (unknown) fits with the ATR information. The differences between expected and real result around 3300cm^{-1} are explained by humidity, but as seen in the Theoretical Study polypropylene (pure) present low water absorption so this humidity would remain on the surface.

All this information about both bulks can be now compared with marked material. No important variations are observed in the marks of black bulk, the polymer chain has not suffered degradation. This low variation between black bulk and mark is agreed with previously commented XPS and EDX analysis. Just a decrease in the intensity of 1750cm^{-1} peak due to the thermal is observed and can be due to degradation in the marking process. In case of white bulk, after marking neither appear degradation of the polymer chain; however it shows not only the same variation of 1750cm^{-1} peak but also stronger differences than appeared in black bulk analysis. There is a significant (relative to other variations) increase in the peaks around 1600cm^{-1} and the wide peak/zone of 3300cm^{-1} . If other bands for C=O would appear, then the variation around 3300cm^{-1} could be explained by oxidation process; but it does not happen and so humidity variations is other probable reason although this material (pure) present low water absorption. Focusing on the variation around 1600cm^{-1} there are various possible explanations like the migration of the additive to the surface, it would increase the additive proportion and it also would explain the changes around 3300cm^{-1} . A second possible explanation is the removal (ablation) of the polypropylene but not of the additive. Also a carbonization process that enhances the aromatic peaks around 1600cm^{-1} is possible, although the expected increase around $700\text{-}900\text{cm}^{-1}$ does not appear. Finally the most probable situation is a combination of all these effects. The higher variations for white bulk before and after marking than the appeared with black bulk are agreed with XPS study presented above. The variations before and after marking are more intense in the XPS study, it could be explained because of the chemical variations are related to the depth of the study. XPS collect information just in the outer-most layers of the sample (3-10 nm) and ATR between 0.5 and 5 μm . So finally ATR shows interesting and fast results but XPS is preferable.

9.6 Elemental analysis (EA)





The quantification of hydrogen has been a problem in all the previously explained experiments; an elemental analysis solves this problem. The most common form of EA is accomplished by combustion analysis. The experimental results (%weight) achieved for this work have been: Pure PP (85.62%C, 15.10% H), white bulk (76.58%C, 14.67%H) and black bulk (77.84%C, 14.49%H).

10 MARK RESISTANCE

10.1 Introduction

The need for an approved laser mark in industrial products comprises mainly color and durability of the mark. The experimental work (*Table 8*) shows that laser marks usually improve the industrial standard tests when compared with marks by tampography. But even overcoming these tests, sometimes the visual appearance can be altered due to surface changes (39).

Table 8: standard tests results achieved in B.S.H. Vitoria

Original mark		Tampography	355nm laser mark
UNE EN 60335-1	The mark has to keep the color after 15s of rubbing with gasoline		
UNE EN ISO2409	The mark has not to be removed with adhesive tape		

Marring: A change in gloss is produced due to topographical modifications of the order of visible light wavelengths. Marring is analyzed with optical characterization (*Chapter 11*).

Scratching: Deep trenching ($\geq 10\mu\text{m}$) with plastic deformation; sometimes it is also accompanied by brittle failure, or other attributes such as scratch whitening. Whitening is a change in the distribution of wavelength and intensity of reflected or scattered light, enhancing scratch visibility. Scratch is related to mechanical properties.

The study of bulk surface or coatings by mean of scratch tests is object of literature discussions (40-44). A relation between mark hardness or scratch resistance and the kind of phenomenon (e.g. foaming) is expected. Common hardness tests for polymers are Rockwell (harder polymers) or Shore (45); this last one has been tested in laser marks and bulk for the present work. For further research improving bulk hardness literature recommend modifications on fillers content or type like wollastonite (41,46) or calcium carbonate (47), or the use of antiscratch additives.

10.2 Shore hardness

The measured property is depth of penetration with a specified penetrator and loads. The experimental study has been made according to the normative *ISO_7619-1=2010* with a durometer type D, value acquired 15s after indentation (coded as D15) and at 21°C. The sample thickness must be as minimum 6mm, but it is possible to use two thinner samples at once. This last question is problematic because a marked layer is in the order of micrometers and the results are then modified by bulk. Using the same bulk the marks have been compared considering this modification as normalization, and also has been compared with bulk hardness. As an example four marks on white PP are shown (*Figure 30*), each measure have been repeated 5 times and standard deviation is shown. The foamings (2500 and 3000 mm/s) have lower Shore hardness than carbonized marks (600 and 1000 mm/s) and are easier to scratch.

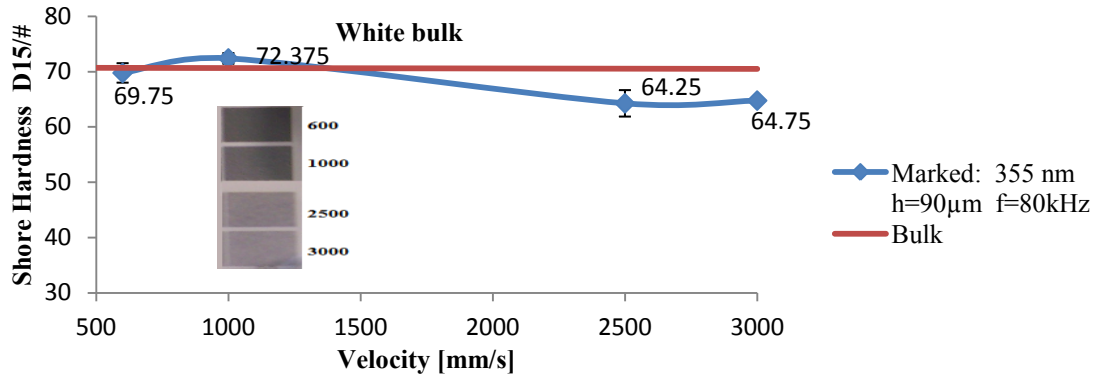


Figure 30: Shore hardness of 4 marks. Foaming hardness is minor than bulk material.

10.3 Scratch Test

Scratch tests are the most interesting tests for mark resistance purposes; marked products suffer mechanical stresses during their lifetime with similar characteristics to these tests. In a scratch test an indenter tip is loaded and a relative movement between indenter and sample produces the scratch (Figure 31).

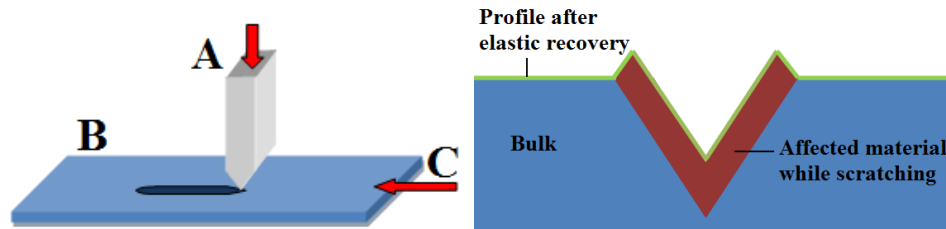


Figure 31: (left) Scratch test elements A: Normal Load B: Sample C: Sample movement. (right) Main parts of scratch cross section profile.

There is an intense discussion (40-44) about scratch tests in literature, mostly about quantification formulas and also about experimental parameters like load value, load type (constant or variable), tip material, tip shape, time, etc (Table 9). Most researchers [CITA] use two cross section measures: profile residual depth and profile scratch width (Figure 31).

Tabla 9: scratch test compilation (39)

TEST	TIP MATERIAL	TIP GEOMETRY	LOAD	SPEED
ASTM	Steel	U Shaped loop 3.25mm \varnothing	0-98N	6mm/s
AFM	Diamond	90° cone 2µm or 2mm \varnothing	50µN-4mN	35-
Ford	Steel	sphere 1mm \varnothing	0.6-30N	100mm/s
Constand Load	Diamond	Berkovich pyramid	1-7N	500µm/s
Progressive Load	Diamond	sphere 4µm \varnothing	0-5mN	5µm/s
Progressive Load	Diamond	sphere 400µm \varnothing	0.5-10N	200µm/s
Progressive Load	Diamond	sphere 20µm \varnothing	0-190mN	50µm/s
Progressive Load	Diamond	60° cone 2-6 µm \varnothing	0-8mN	25µm/s
Progressive Load	Diamond	Berkovich pyramid	0.02-16mN	10-
Progressive Load	Diamond	Cube corner pyramid 1-	0.02-16mN	25µm/s

Researchers seem to conclude that smaller scratch scale results like the ones achieved with nanoindenter devices are more accurate and that AFM is the best device for these tests. At the same time automobile companies offer macroscopical methodologies that are less accurate but easier to implementation. After the firsts experiments for this work nanoindenter confirmed a disadvantage when applied to laser marks of polymers. Marks are commonly rough, containing multiple craters or grooves. The size of these defects compared with the nanotip avoid a proper measurement, results are disperse and dependent on position and direction of scratch test. The result cannot be representative for the full mark. An example is presented below (*Figure 32*).

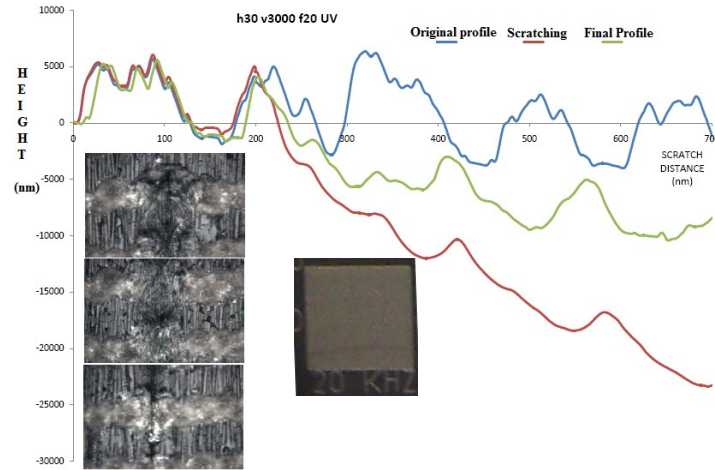


Figure 32: the graphic shows the original surface profile (blue), the profile during scratching with increasing load (red) and the residual profile after the scratch (green). The same test, but testing parallel to marking direction (horizontal grooves) produces a non comparable result.

So this test is recommended for smooth surface textures, the scratch direction has to be considered due to the possibility of directional textures (e.g. grooves).

On the other hand it has been experimented with the Erichsen method using a Volkswagen tip 1mm Ø. This device (*Figure 35*) is similar to a traditional pen; firstly the researcher introduces a spring in the device, it allows work in a range of forces (see *Figure 33* red and yellow dots). The second step consists into select a force value in this range. The researcher moves the device like as writing with a pen, if the material is not scratched a higher value of force is selected and the process repeated until the scratch appears. All scratch results for marks on PP random (various colors) achieved for this work have been between 1 and 5N. For improved accuracy the scratch groove can be measured (depth, width) and not only observed.

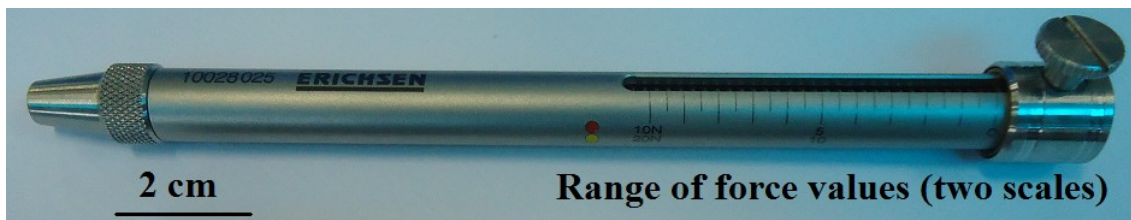


Figure 35: scratch Erichsen test, two springs allow force values between 0 and 20N

11 OPTICAL CHARACTERIZATION

11.1 Introduction

It is desired to know the absorption or the optical density (OD=absorption/distance unit) of the bulk at the selected wavelength because it is the cause of almost every phenomenon taking place while laser marking. Once the material is marked the researcher also requires an objective color measurement of the marks and the bulk.

11.2 Spectra

An optical analysis of the bulk includes the transmission and/or reflection spectra of bulk; with them the researcher calculates the absorption at the laser wavelength used for marking (*Figure 34*). Once the light is absorbed it can suffer of scattering, it focuses (hot spots) or disperses the laser beam. Scattering analysis includes the search of material scattering properties (36), surface roughness and various spectra using integrating sphere and light traps, this type of study is not developed in this work.

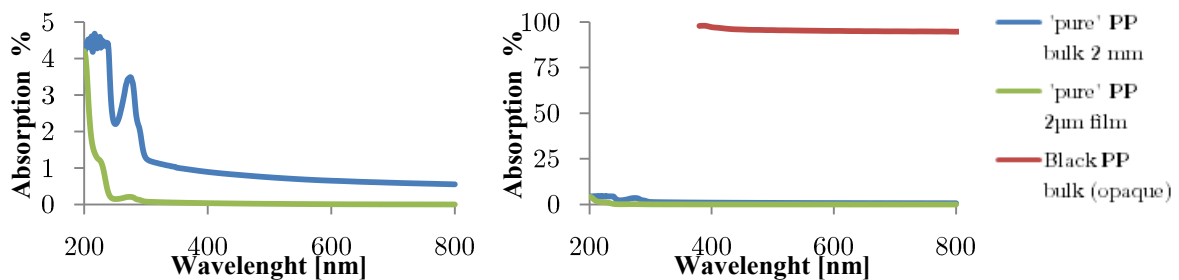


Figure 34: (left) Absorption of pure PP for two different thicknesses calculated by mean of a transmission spectrum IR-UV (right) Same graphic adding the absorption of black PP bulk calculated by mean of two reflection spectra, with and without specular component.

11.3 Color

Other important concept about optical characterization is the human perception of color; the visible spectrum detected by human eyes is in a range between 380 and 780nm. Moreover with the aim to compare colors a quantification (color coordinates) is required. The CIE (*International Commission on illumination*) has been working on human color perception since 1931. Four main concepts must be considered (48):

Standard observer: the foveal system of the human eye is the only part of the retina that permits 100% visual acuity. Based on this concept CIE established the fields of view *CIE1931* (2°) and *CIE1967* (10°) for standard observers (*Figure 35*). Moreover the standard observer is characterized by three color matching functions, which describe observer chromatic response.

Measurement geometry: the specular component of reflection provides information about the illuminant and the diffuse component of reflection provides information about the color. CIE recommends 4 measurement geometries (illuminant/observer): $45^\circ/0^\circ$, $0^\circ/45^\circ$, Diffuse/ 0° and

0° /Diffuse (*Figure 35*). Diffuse conditions are obtained by mean of integrating spheres. When comparing colors similar measurement conditions are recommended, considering $45^\circ/0^\circ$ and $0^\circ/45^\circ$ as equivalent.

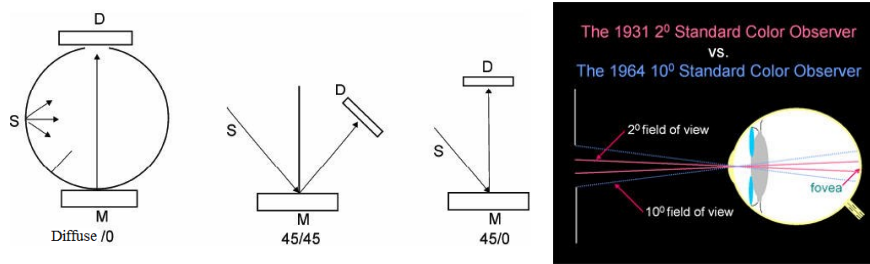


Figure 35: (left) Various measurement geometries (S°/D°) for sample M. (right) Standard photometric observer [Source www.cyberchromeusa.com]

Standard illuminant: standards D (Daylight) illuminants are commonly used, mostly D65 and D50 (*Figure 36*). The numeration is related to the black body temperature which provides the same spectra, for example D65 and 6500K. D65 is similar to a mid-day sun in Europe with covered sky, D50 is similar to direct solar light and provides a more uniform spectra.

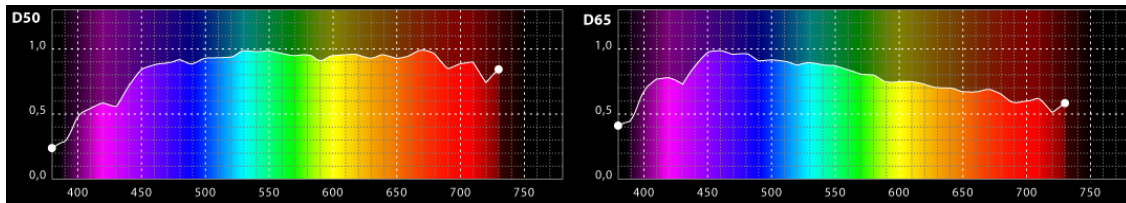


Figure 36: standards D65 and D50 relative energy and wavelength [Source: www.gusgsm.com]

White reference (perfect light diffuser): the same color is observed independently from the observer and light position. It is only an idealization and white ceramic calibrated plates are used.

Once these four conditions are established the concept of color coordinates can be explained. Coordinates are related to a chromaticity space, for this work *CIE1976 $L^*a^*b^*$ space* (a.k.a. CIELAB) based in XYZ stimulus is used because of its approximation to human perception and common use in literature; other spaces are for example CYMK or RGB. CIELAB space is usually represented as a sphere where vertical coordinate (L^*) considers lightness (cube root of the relative luminance) and moves between black '0' and diffuse white '100'. Horizontal coordinate a^* is between red (magenta) and green and horizontal coordinate b^* is between blue and yellow (*Figure 37*). Once the color is placed in $L^*a^*b^*$ coordinates a comparison between colors (e.g. bulk and mark) is commonly required. The formulas of color distance are intended to imitate the nonlinear response of the eye. Since 1976 in literature different formulas have been discussed, this work recommends CIEDE2000 (a.k.a. ΔE_{00}) according to (49-51). Michelson Contrast (a.k.a. visibility) is other commonly used formula considering just L coordinate. *Figure 38* shows a comparison between Michelson Contrast and ΔE_{00} for various marks, can be observed that when having black, white and grey colors both graphics have similar shape. At this point the researcher must acquire the color coordinates; various devices with different characteristics are available.

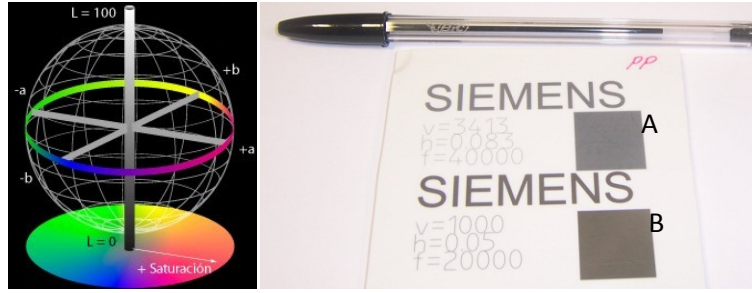


Figure 37: (left) CIELAB color space [Source: www.gusgsm.com] (right) Image of marks A and B in white bulk whose color analysis appears in Table 10

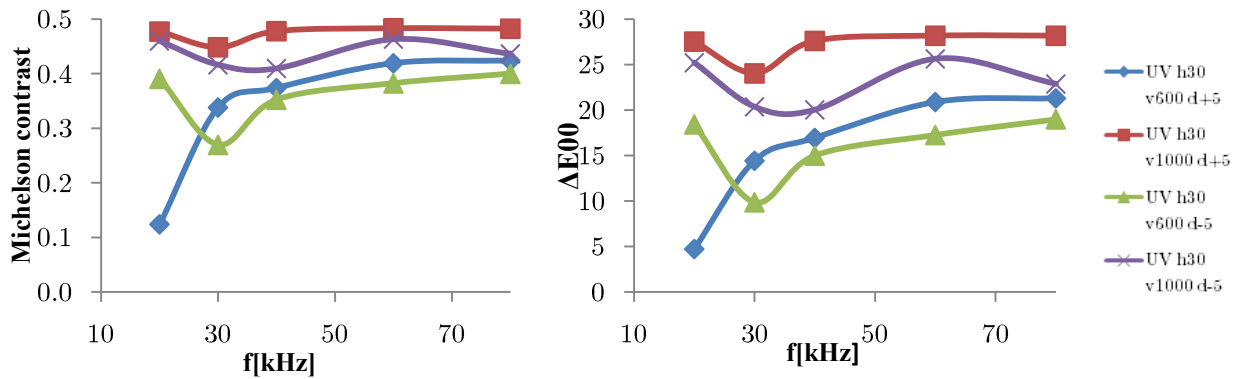


Figure 38: comparison of Michelson Contrast and ΔE_{00} for various foamings of black bulk. Color coordinates achieved with I1basicPro spectrophotometer

Spectrophotometers get information with high accuracy, working each few nanometers; however colorimeters and calibrated cameras using RGB detectors show with minor precision. When using a camera a standard cabin with uniform and diffuse normalized light is needed; the image can be post processed obtaining information at pixel level. In a similar manner to Campos Acosta et al (54) three different color measurement devices have been tested for this work and an example is exposed in Table 16, moreover the related photos are shown in Figure 37. Because of different measurement conditions light variations (differences ≤ 1 are not perceived) in color coordinates are observed; color distance and contrast results are comparable for all devices.

Table 16: $L^*a^*b^*$ coordinates, ΔE_{00} and Michelson contrast for white bulk and 355nm laser marks A) 3413 v [mm/s] 40 f[kHz] 0,08 h[μ m] and B) 1000 v [mm/s] 20 f[kHz] 0,05 h[μ m]

	Mark	L	a	b	Michelson	ΔE_{00}	Light	Measurement
Espectrophotometer I1BasicPro	A	49,17	-1,40	-1,90	0,30	32,27	D50	0°
	B	43,90	1,10	5,20	0,35	38,09	D50	0°
	bulk	90,88	-1,50	-0,95			D50	0°
Colorimeter Konica Minolta CM-700d with integrer sphere	A	47,73	-1,11	-1,58	0,31	33,58	D65	0°
	B	42,93	0,83	5,38	0,36	38,78	D65	0°
	bulk	90,69	-0,99	0,08			D65	0°
Goniospectrophotometer MacBeth Auto-eye 642	A	49,10	-0,80	-1,50	0,30	32,55	D65	0°
	B	43,10	0,50	5,10	0,36	38,82	D65	0°
	bulk	91,20	-1,00	0,20			D65	0°

Colors can be defined following the previously explained experimental conditions, but the perception of color varies with other conditions (e.g. metamerism) and because of specific textures or effect pigments. *Figure 39* shows with an example the differences between color and its perception. According to these concepts integrating spheres are interesting when comparing materials with different textures or different glossy level (perception)but have a disadvantage when comparing color; A goniospectrophotometer (*Figure 40*) is of interest when comparing the perception of polymers with metal, glitter, pearl or sparkle effects.

Finally a visual inspection is recommended before accepting the quality of a mark. These inspections are realized using a standard cabin (*Figure 39*), a normalized color palette for comparisons and various human observers.

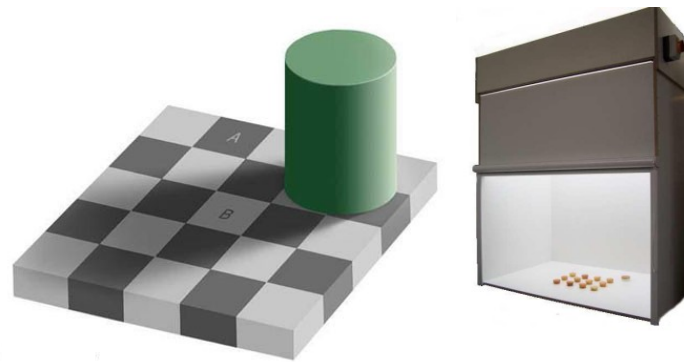


FIGURE 39: (left) A and B have the same color but the background changes human perception [Source: Edward H.Adelson]. (right) Standard cabin used in B.S.H. Zaragoza

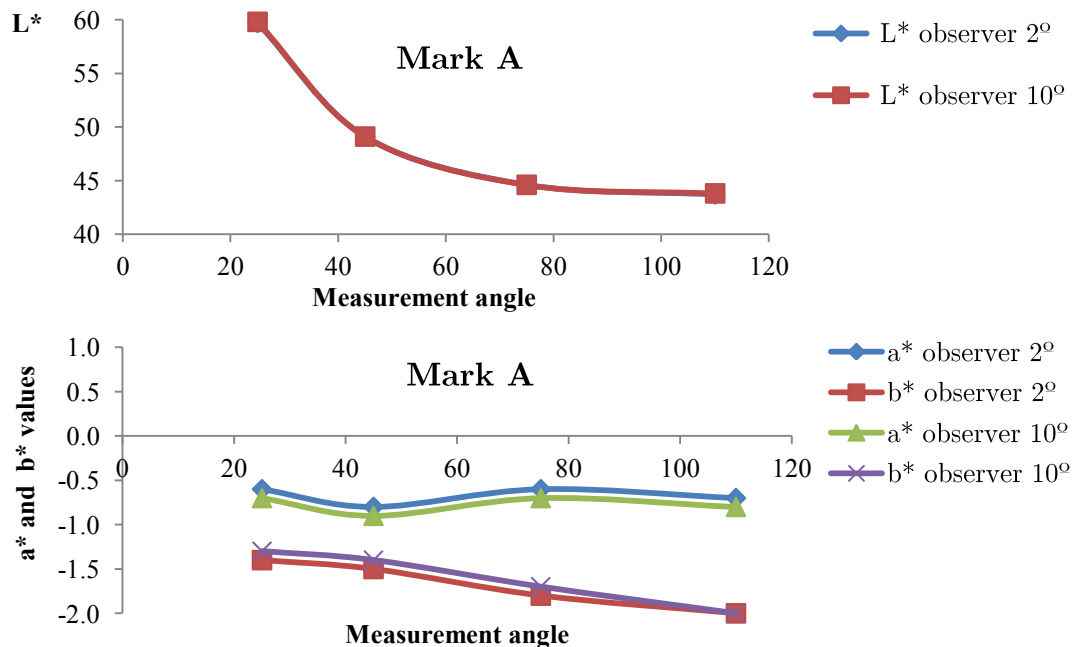


Figure 40: comparison of goniospectrophotometer results related to standard observer field (2°, 10°) and measurement angles (25°, 45°, 75°, 110°) for mark A. Illuminant angle is fixed at 45°.

12 CONCLUSION

Along the present work numerous methods and devices have been tested according to the state of art of various research fields, all of them related to laser or polymers. The proposed experimental examples allow accepting, adapting or discarding the devices or work methods. The conclusion of this work is a work methodology that is resumed below (*Figure 41*):

Firstly the researcher needs a previous knowledge about the state of art of laser marking and polymer properties. A factorial design of the experiments allows determining the importance of each parameter of study. In this work the recommended laser parameters are velocity, frequency, pump power, distance between lines and distance between lens and sample.

Before marking, the samples have to be produced; it has been explained that the quantitative and qualitative control of the material content is an important question for further experiments. The sample size has to allow numerous marks in form of matrix and it is preferred low time for samples production. Injection molding has shown all these characteristics and a laboratory press molding device is appropriate for the production of a few first samples. These few samples can be produced before injection to test new additives whose response to laser is unknown.

Most of phenomena taking place in the material are due to the absorption of energy, it has to be measured with spectrophotometers for the laser wavelength. In the case of transmission spectra the optical density related to an absorption value is also a main question.

An accurate measurement of the temperature in real time for an area of a few microns is an unsolved challenge. Mathematical simulations are interesting for thermal ablation processes.

Confocal has demonstrated the best results for morphology studies. It is able to produce 2D profiles, 3D mapping, photographs and direct roughness measurement for wide areas. A 10x lens is enough to represent the evolution of roughness related to the evolution of a laser parameter.

The knowledge about the interaction between the laser beam and the polymer requires identifying the elementary content of each component of the material (e.g. additives), the bulk and the marks. XPS has shown the best results including the determination of atomic percent for all the elements of interest with the exception of hydrogen. This device also allows determining the bondings for each element. ATR analysis fulfills the XPS study.

The aim of laser marking is to replace other marking processes as tampography and so the marks require high resistance and color contrast. Scratch test methods using nanoindenter are being discussed in literature. This type of test has shown confusing results for laser marks with texture size similar to the size of the tip. Erichsen method is less accurate according to the literature but it is an advantage for the analysis of the laser marks.

Finally the researcher requires to identify bulk and mark color, it has been explained how to obtain color coordinates according to CIE requirements. Different devices and measurement conditions have shown similar results and the same values of color distance between bulk and mark.

At the same time that the work methodology is established the experimental examples offer useful information about a variety of materials. The work is mainly focused in polypropylene with diverse additives and pigments; the foremost phenomena of the interaction between the laser beam and the polypropylene compounds have been studied. Furthermore it has been achieved good quality marks on PP, ABS and SAN which are expected to be used in commercial products in 2012.

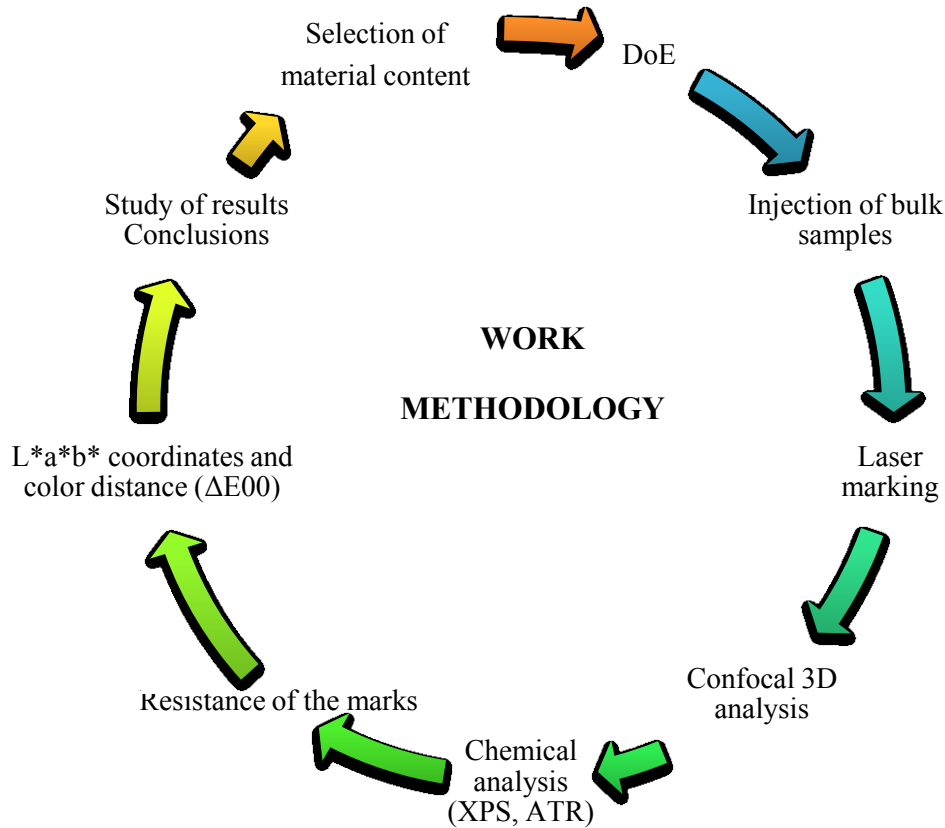


Figure 41: work methodology schema

13 FUTURE

This work methodology is expected to be used systematically for various researchers; it fits with the usual conditions of polymer marking but can also be adapted for new situations; new devices or methods can be added to the methodology. Raman, analysis of gases, Brinell hardness or measurement of stress waves (9,22) are analysis proposed for the future. In addition new atmospheres (water, nitrogen), obtaining functional textures or the development of additives for enhanced laser marking are suggested. On the other hand diverse ideas and results are being patented at the moment of publish this work and it is expected to publish related articles in a near future.

Other possibilities of study about the interaction between lasers and polymers are open, for example a textured polymer could be used as substrate for cellular growth or ablation can be used to produce polymer lenses.

BIBLIOGRAPHY

- (1) Lippert T, Wei J, Wokaun A, Hoogen N, Nuyken O. *Polymers designed for laser microstructuring. Appl Surf Sci* 2000 12/15;168(1-4):276-272.
- (2) Casalino G, Ghorbel E. *Numerical model of CO2 laser welding of thermoplastic polymers. J Mater Process Technol* 2008 10/16;207(1-3):65-71.
- (3) Acherjee B, Kuar AS, Mitra S, Misra D. *Effect of carbon black on temperature field and weld profile during laser transmission welding of polymers: A FEM study. Optics & Laser Technology* 2012 4;44(3):514-521.
- (4) Chen M, Zak G, Bates PJ. *Effect of carbon black on light transmission in laser welding of thermoplastics. J Mater Process Technol* 2011 1/1;211(1):45-47.
- (5) Acherjee B, Kuar AS, Mitra S, Misra D. *Effect of carbon black on temperature field and weld profile during laser transmission welding of polymers: A FEM study. Optics & Laser Technology* 2012 4;44(3):514-521.
- (6) - *Polymer ablation: From fundamentals of polymer design to laser plasma thruster. - Applied Surface Science (- 15):- 6409.*
- (7) Laude LD, Martinez D, Dicara C, Hanus F, Kolev K. *The ablation of polymers under excimer laser irradiation: the physics of the process and the polymer structure. Nuclear Instruments and Methods in Physics Research Section B: Beam Interactions with Materials and Atoms* 2001 12;185(1-4):147-155.
- (8) Chang T, Molian PA. *Excimer pulsed laser ablation of polymers in air and liquids for micromachining applications. J Manuf Syst* 1999;18(2, Supplement 1):1-17.
- (9) Sato H, Nishio S. *Polymer laser photochemistry, ablation, reconstruction, and polymerization (REVIEW) . Journal of Photochemistry and Photobiology C: Photochemistry Reviews* 2001 12/13;2(2):139-152.
- (10) Krüger J, Kautek W. *Ultrashort pulse laser interaction with dielectrics and polymers. Polymers and Light* 2004;247-290.
- (11) Aguilar CA, Lu Y, Mao S, Chen S. *Direct micro-patterning of biodegradable polymers using ultraviolet and femtosecond lasers. Biomaterials* 2005 12;26(36):7642-7649.
- (12) Duy Pham and Livia Tonge and Jinan Cao and Jon Wright and Michal Papiernik and Erol Harvey and, Dan Nicolau. *Effects of polymer properties on laser ablation behaviour. Smart Mater Struct* 2002;11(5):668.
- (13) Dieter Bauerle. *Laser processing and chemistry. 4th ed.: Springer.*
- (14) Evonik Industries. *Polymers & Lasers Laser Application Center.*
- (15) LATI Industria. *Laser marking on thermoplastics.*
- (16) DSM Engineering plastics. *General information on laser marking of DSM engineering plastics.*

- (17) Zheng H, Lim GC. Laser-effected darkening in TPEs with TiO₂ additives. *Optics and Lasers in Engineering* 2004 5;41(5):791-800.
- (18) Ricciardi G, Cantello M, Aira GS. Marking of Computer Keyboards by Means of Excimer Lasers. *CIRP Ann Manuf Technol* 1996;45(1):191-196.
- (19) Zheng HY, Rosseinsky D, Lim GC. Laser-evoked coloration in polymers. *Appl Surf Sci* 2005 5/30;245(1-4):191-195.
- (20) Fukumura H, Hatanaka K, Hobley J. Laser light interactions with organic solids and their surfaces. *Journal of Photochemistry and Photobiology C: Photochemistry Reviews* 2001 12/13;2(2):153-167.
- (21) Bormashenko E, Pogreb R, Sheshnev A, Shulzinger E, Bormashenko Y, Sutovski S, et al. Thermal degradation of thermoplastic and thermosetting polymers induced by laser radiation and its study by FTIR spectroscopy. *Polym Degrad Stab* 2001;72(1):125-131.
- (22) Esposito E, Scalise L, Tornari V. Measurement of stress waves in polymers generated by UV laser ablation. *Optics and Lasers in Engineering* 2002 10;38(5-4):207-215.
- (23) Daniel Sola. *Mecanizado láser de materiales cerámicos y vitrocerámicos*. Zaragoza: Universidad de Zaragoza; 2010.
- (24) Feng Y, Liu ZQ, Yi X-. Co-occurrence of photochemical and thermal effects during laser polymer ablation via a 248-nm excimer laser. *Appl Surf Sci* 2000 2/2;156(1-4):177-182.
- (25) Joan Ferré. *El diseño factorial completo 22*. Grupo de Quimiometría y Cualimetría Departamento de Química Analítica y Química Orgánica Universidad Rovira i Virgili (Tarragona).
- (26) Enrique Yacuzzi (Universidad del CEMA) Fernando Martín (Aventis Pharma) Hugo Marcelo Quiñones (Universidad del CEMA) Matías Julián Popovsky (Universidad del CEMA). *El diseño experimental y los métodos de Taguchi: conceptos y aplicaciones en la industria farmacéutica*.
- (27) Bogaerts A, Chen Z, Gijbels R, Vertes A. Laser ablation for analytical sampling: what can we learn from modeling? *Spectrochimica Acta Part B: Atomic Spectroscopy* 2003 11/21;58(11):1867-1893.
- (28) Koukoulis IN, Provatidis CG, Georgiou S. Finite element modeling of the mechanical effects of the UV laser ablation of polymer coatings. *Appl Surf Sci* 2008 3/30;254(11):3531-3539.
- (29) Arnold N, Bityurin N, Bäuerle D. Laser-induced thermal degradation and ablation of polymers: bulk model. *Appl Surf Sci* 1999 1;138-139(0):212-217.
- (30) Bityurin N, Arnold N, Luk'yanchuk B, Bäuerle D. Bulk model of laser ablation of polymers. *Appl Surf Sci* 1998 5;127-129(0):164-170.
- (31) Sinkovics B, Gordon P, Harsányi G. Computer modelling of the laser ablation of polymers. *Appl Therm Eng* 2010 11;30(16):2492-2498.

- (32) Rebollar E, Bounos G, Oujja M, Georgiou S, Castillejo M. Morphological and chemical modifications and plume ejection following UV laser ablation of doped polymers: Dependence on polymer molecular weight. *Appl Surf Sci* 2007 7/31;253(19):7820-7825.
- (33) Anita J. Brandolini, Deborah D. Hills. *NMR spectra of polymers and polymer additives*. EEUU: Marcel Dekker; 2000.
- (34) Resano M, García-Ruiz E, Vanhaecke F. Laser ablation-inductively coupled plasma-dynamic reaction cell-mass spectrometry for the multi-element analysis of polymers. *Spectrochimica Acta Part B: Atomic Spectroscopy* 2005 11;60(11):1472-1481.
- (35) Todolí J-, Mermet J-. Study of polymer ablation products obtained by ultraviolet laser ablation — inductively coupled plasma atomic emission spectrometry. *Spectrochimica Acta Part B: Atomic Spectroscopy* 1998 10/28;53(12):1645-1656.
- (36) Michael Bolgar, Jack Hubbal, Joe Groeger, Susan Meronek. *Handbook for the chemical analysis of plastic and polymer additives*. : CRC Press; 2008.
- (37) Patrick Rudewicz and Burnaby Munson. *Determination of Additives in Polypropylene by Selective Chemical Ionization Mass Spectrometry*. 1986.
- (38) H. El Mansouri* / N. Yagoubi / D. Ferrier. *Extraction of Polypropylene Additives and Their Analysis by HPLC*.
- (39) Mark R. VanLandingham. *Scratch and Mar Resistance of Polymeric Materials*. U S Army Research Laboratory .
- (40) Brun C, Delobelle P, Fromm M, Berger F, Chambaudet A, Jaffiol F. Mechanical properties determined by nanoindentation tests of polypropylene modified by He+ particle implantation. *Materials Science and Engineering: A* 2001 9/30;315(1-2):65-69.
- (41) Hadal R, Dasari A, Rohrmann J, Misra RDK. Susceptibility to scratch surface damage of wollastonite- and talc-containing polypropylene micrometric composites. *Materials Science and Engineering: A* 2004 8/25;380(1-2):326-339.
- (42) Busico V, Cipullo R. Microstructure of polypropylene. *Progress in Polymer Science* 2001 4;26(3):445-533.
- (43) Friedrich K, Sue HJ, Liu P, Almajid AA. Scratch resistance of high performance polymers. *Tribol Int* 2011 8;44(9):1032-1046.
- (44) Wong M, Lim GT, Moyses A, Reddy JN, Sue H-. A new test methodology for evaluating scratch resistance of polymers. *Wear* 2004 6;256(11-12):1214-1227.
- (45) Sahin S, Yayla P. Effects of testing parameters on the mechanical properties of polypropylene random copolymer. *Polym Test* 2005 8;24(5):615-619.
- (46) Dasari A, Rohrmann J, Misra RDK. On the scratch deformation of micrometric wollastonite reinforced polypropylene composites. *Materials Science and Engineering: A* 2004 1/15;364(1-2):357-369.

(47) Zokaei S, Lesan Khosh M. R, Bagheri R. Study of scratch resistance in homo- and co-polypropylene filled with nanometric calcium carbonate. *Materials Science and Engineering: A* 2007 2/15;445-446(0):526-536.

(48) Edison Valencia Díaz. *Procesado de imagen digital en color: Adquisición, Análisis Colorimétrico y Realce*. Universitat Politècnica de Catalunya. Departament d'Òptica i Optometria; 2007.

(49) Gaurav Sharma, Wencheng Wu, Edul N. Dalal. *The CIEDE 2000 color-difference formula: Implementation notes, supplementary test data and mathematical observations*. 2004.

(50) Manuel Melgosa. *Testing CIELAB based color difference formulas*. *Color research and application* 1999.

(51) M. Melgosa, E.Hita, M.M. Perez, J.A. Martinez. *Recientes análisis sobre la fórmula de diferencia de color CIE94*. *Optica pura y aplicada* 1996.

(52) Shaochen Chen and Costas P. Grigoropoulos *Noncontact nanosecond-time-resolution temperature measurement in excimer laser heating of N-P disk substrates* 1997

(53) www.insht.es Ministry of employment and social security

(54) Campos Acosta, J.; Rubiño López, M.; Castillo Rubí, F. y Pons Aglió, A. *Colour Measurement Instruments Comparison*. *ÓPTICA PURA Y APLICADA – Vol. 37, núm. 1, - 2004*

LIST OF PATENTS RELATED TO THE PRESENT WORK

In order to resume the information just the publication numbers are shown, the full information can be found in www.espacenet.com . All these patents are in Spanish, English or German language; Other patents (e.g. Japanese) have been excluded.

Publication number

DE10053639 (A1)	US2001030179 (A1)	DE102006046628 (A1)	WO2006029677 (A1)
US2010156001 (A1)	US2001021731 (A1)	DE102006026789 (A1)	US2006074165 (A1)
US2010196698 (A1)	ES2342592 (T3)	DE102004050571 (A1)	EP1431050 (A2)
DE102004053376 (A1)	US6214917 (B1)	DE10324488 (A1)	DE102004026335 (A1)
DE10034472 (A1)	US6521688 (B1)	DE10243005 (A1)	DE102007002786 (A1)
DE19942316 (A1)	US5928780 (A)	DE10237732 (A1)	EP1817368 (A1)
US6284184 (B1)	US2010181754 (A1)	DE20023710 (U1)	DE19944372 (A1)
EP0684144 (A1)	WO2009090057 (A1)	DE10053771 (A1)	EP1350818 (A1)
CA2111162 (A1)	WO2009049805 (A1)	DE19832733 (A1)	US2004101671 (A1)
IE910266 (A1)	DE102004027622 (A1)	DE19811028 (A1)	US2002107305 (A1)
CA1281546 (C)	CA1284125 (C)	DE19541453 (A1)	DE19753248 (A1)
US2006260481 (A1)	EP1897699 (A2)	DE19517625 (A1)	DE19646332 (A1)